FINAL REPORT

STUDIES CONCERNING ENHANCEMENT OF CONDUCTIVITY OF POLYMER ELECTROLYTES AND STABILITY OF LITHIUM ANODES

SPONSORED BY

EUROPEAN OFFICE OF AEROSPACE RESEARCH AND DEVELOPMENT
UNITED STATES AIR FORCE
LONDON

CONTRACT NO. F61708-95-C0007

INVESTIGATOR
DR. N. MUNICHANDRAIAH

FEBRUARY 1997

DEPARTMENT OF INORGANIC AND PHYSICAL CHEMISTRY
INDIAN INSTITUTE OF SCIENCE
BANGALORE-560012
INDIA

DISCLAIMER NOTICE

THIS DOCUMENT IS BEST QUALITY AVAILABLE. THE COPY FURNISHED TO DTIC CONTAINED A SIGNIFICANT NUMBER OF PAGES WHICH DO NOT REPRODUCE LEGIBLY.

REPORT DOCUMENTATION PAGE

Form Approved OMB No. 0704-0188

1. AGENCY USE ONLY (Leave blank)	2. REPORT DATE	3. REPORT TYPE AND DATES COVERED
	14 February 1997	Final Report

4. TITLE AND SUBTITLE

Studies Concerning Enhancement of Conductivity of Polymer Electrolytes and Stability of Lithium Anodes

5. FUNDING NUMBERS

F6170895C0007

6. AUTHOR(S)

Dr. Nookala Munichandraiah

7. PERFORMING ORGANIZATION NAME(S) AND ADDRESS(ES)

Indian Institute of Science
UGC Center of Advanced Study
Bangladore 560 012
India

8. PERFORMING ORGANIZATION REPORT NUMBER

N/A

9. SPONSORING/MONITORING AGENCY NAME(S) AND ADDRESS(ES)

EOARD
PSC 802 BOX 14
FPO 09499-0200

10. SPONSORING/MONITORING AGENCY REPORT NUMBER

SPC 95-4002

11. SUPPLEMENTARY NOTES

12a. DISTRIBUTION/AVAILABILITY STATEMENT

Approved for public release; distribution is unlimited.

12b. DISTRIBUTION CODE

A

13. ABSTRACT (Maximum 200 words)

This report results from a contract tasking Indian Institute of Science as follows: The contractor will investigate the passivation process that can result in increased charge transfer and thin film resistance at the lithium electrode polymer electrolyte interface.

14. SUBJECT TERMS

Chemistry

15. NUMBER OF PAGES

90

16. PRICE CODE

N/A

17. SECURITY CLASSIFICATION OF REPORT	18. SECURITY CLASSIFICATION OF THIS PAGE	19. SECURITY CLASSIFICATION OF ABSTRACT	20. LIMITATION OF ABSTRACT
UNCLASSIFIED	UNCLASSIFIED	UNCLASSIFIED	UL

STUDIES CONCERNING ENHANCEMENT OF CONDUCTIVITY OF POLYMER ELECTROLYTES AND STABILITY OF LITHIUM ANODES

1. INTRODUCTION

Electrochemical power sources, which are commonly known as batteries, have occupied prime importance in the area of energy storage and supply. These devices convert chemical energy into electrical energy and are under use for a wide range of applications in consumer as well as large-scale industrial market.

Schematically, a battery consists of a positive electrode and a negative electrode in a suitable electrolyte. When an electric load is connected across the two terminals of the battery, electrooxidation of the chemical at the negative electrode takes place thereby electrons are released to the external circuit. Electrons travel through the load, thus performing the electrical work, and reach the positive electrode in the battery. The positive electrode material consume the electrons and undergo a reduction process. Current is carried inside the battery by transport of ions. The oxidation and reduction processes at the negative and the

positive electrodes respectively, take place simultaneously when the battery is under discharge. The net free energy decrease of these reactions is manifested in the form of electrical energy. When a rechargeable battery is subjected to charging, the reverse electrochemical processes take place within the battery.

An important parameter reflecting usefulness of a battery for a given application is the specific energy, i.e., energy output per unit weight or unit volume of the battery, usually in the units of Wh kg^{-1} or Wh l^{-1} respectively. The present global research and developmental efforts in this field are oriented to improve the specific energy of known battery systems as well as to develop new battery systems with high specific energy. Lithium-based battery system are emerged as high energy batteries because of the following reasons [1-3]: Lithium is a very light metal with density 0.51 g cc^{-1}. Since its atomic weight is 6.94, the specific capacity as an electrode is as high as 3.86 Ah g^{-1}. This value is the highest of all the known metal electrodes. The electrode potential being -3.03 V, a battery employing lithium electrode in a non-aqueous electrolyte has a cell voltage in the range of 3-4 V. These factors are responsible for realizing a high specific energy (100-120 Wh kg^{-1}) of lithium based batteries.

1.1. The importance of Li/solid polymer electrolyte system

Although primary batteries based on lithium electrode are commercially realized during the last two decades, development of rechargeable Li batteries with high specific energy and long cycle life remained a difficult task. Recent development and commercialization of lithium-ion cells is a step forward in this direction.

Development of a rechargeable Li battery which employs a solid polymer as an electrolyte has been of top most interest in recent years. By replacing the conventional liquid non-aqueous electrolyte with a solid polymer electrolyte (SPE) film, several advantages are expected : (i) The SPE is very thin (a few tens of microns thick) and therefore the internal voltage drop is minimum during the operation of the battery. (ii) As the electrolyte is in the form of a solid film, it acts also as a separator in addition to its normal function as an ionic conductor. Thus, there is a reduction in the number of cell components, viz., the separator and hence reduction in weight of the battery. (iii) The reactivity of Li and other cell components in the solid electrolyte are anticipated to be relatively less aggressive than in liquid electrolyte. Therefore, problems related to passive film formation on Li are likely to be less serious. (iv) The deposition and oxidation of Li is expected to take place uniformly on the Li metal surface without

the formation of dendrites. The first two advantages are expected to contribute for enhancement of specific energy, while the other two advantages contribute for safe and long cycle life of the rechargeable lithium-solid polymer battery.

Consequent upon foreseeing a rechargeable lithium polymer solid state battery with specific energy in the range 150-200 Wh kg^{-1}, tremendous R&D efforts are being expedited worldwide to achieve the goal.

1.2. Objective of the present investigations

There are two key problems to be solved at the forefront of development of the rechargeable lithium-polymer solid state battery.

(i) The specific conductivity (σ) of a solid polymer electrolyte needs to be greater than 10^{-3} S cm^{-1} for applications in a battery. In addition to this prime-requisite, the SPE should be electrochemically stable for long cycle-life of the battery. It should also provide efficient contacts at the electrodes, and needs to facilitate the kinetics of electrochemical reactions at sufficiently higher rates. Additionally the SPE should possess good dimensional stability. Development of a SPE possessing these properties is required.

(ii) Being highly electronegative, lithium is very reactive to air, moisture and other chemical environments. As a result,the surface of lithium metal is covered with an inherent film of the reaction products. The film, known as passivating layer, is

beneficial for primary battery applications. It is, however, detrimental for operation of rechargeable battery. The continuous growth of the passive film, and uneven deposition and oxidation of lithium leading to the formation of lithium-dendrites hamper the electrode performance.

The objectives of the present investigations have been to study the stability of lithium in polymer electrolyte medium and the influence of passivating film on the electrochemical reaction at lithium metal/polymer electrolyte interface. Experiment have been essentially oriented towards studies related to problem (ii) above. Additionally, efforts have been put to prepare a SPE with improved performance, i.e., studies related to problem (i).

2. EXPERIMENTAL ASPECTS

2.1. Chemicals and materials

All chemicals - propylene carbonate (PC), ethylene carbonate (EC), polyethyleneoxide (PEO), polyacrylonitrile (PAN), lithium perchlorate and lithium ribbon (0.75mm thick) were obtained from Aldrich. PEO, PAN and EC were used as received. PC was vacuum distilled and stored over molecular sieves; and $LiClO_4$ was dried under vacuum before using for the experiments.

2.2. Preparation of polymer films

Solid polymer electrolyte films consisting of PEO and $LiClO_4$ were prepared by dissolving the required quantities of PEO and $LiClO_4$ in acetonitrile. The solution was continuously stirred for several hours before casting the films on Teflon covered glass plates and allowing the solvent to evaporate at room temperature. The films were finally dried at 80°C under reduced pressure for about 6 h followed by storing them in a vacuum desiccator. Following this procedure, films of PEO, PEO_4LiClO_4, PEO_8LiClO_4, $PEO_{16}LiClO_4$, $PEO_{32}LiClO_4$ and PEO_8LiClO_4-PC were prepared. Propylene carbonate (PC) was used as a plasticizer to enhance the conductivity of PEO_8LiClO_4 solid polymer electrolyte.

Gel polymer electrolyte films were prepared by dispersing polyacrylonitrile (PAN) in a solution of propylene carbonate (PC) and ethylene carbonate (EC) containing $LiClO_4$. The homogeneous suspension was spread on a glass petri dish preheated to 80°C. Heating was continued for about 5 min. A transparent gel film was formed.

Hybrid solid polymer electrolyte (HSPE) films consisting of PEO and PAN were prepared by first dissolving appropriate quantities of PEO, PC, EC and $LiClO_4$ in acetonitrile. The required quantity of PAN was added and the solution stirred for several hours to ensure uniform dispersion of the undissolved

PAN. A film was cast by spreading the suspension on Teflon covered glass plates and allowing the solvent to evaporate slowly. Finally the film was dried at 80°C under vacuum for about 10 h. The resulting film of HSPE was visually examined for its dry and free-standing nature.

2.3. Assembling of cells

Symmetrical cells of the type SS/SPE/SS and (SS)Li/SPE/Li(SS), where SS refers to stainless steel, were assembled for the investigations. Teflon assemblies, which were provided with stainless steel discs were employed as the cell holders. Polymer film was sandwiched between two discs of lithium (area : 1 cm^2), and held inside the cell holder, which was tightened under mild pressure. All cells were assembled in a dry box filled with argon. While (SS)Li/SPE/Li(SS) symmetrical cells were employed for a majority of the experiments, the SS/SPE/SS cells were used for some experiments needed for conductivity studies.

2.4. Experimental techniques

Majority of the experiments were conducted by using galvanostatic voltage-transient technique and alternating current electrochemical impedance spectroscopy.

The galvanostatic voltage-transient studies were carried out by a direct current circuit consisting of a regulated power supply, a high resistance (500 KΩ) and a galvanometer. The cell voltage was measured by using a digital voltmeter (± 0.1 mV resolution) and/or a Rikadenki X-Y recorder. A constant current in the range from 10 to 50 μA was passed through the cell and voltage changes were measured over a period of 30 min. After completing the measurements by passing a certain magnitude of current, the circuit was opened and the cell was allowed to relax for about an hour under open circuit conditions followed by passing the same magnitude of current in the reverse direction.. The cell was allowed to stand at the open circuit for a few hours before changing the magnitude of current. This procedure ensured equilibrium conditions in the cell before starting an experiment as well as the reproducibility of the data.

Alternating current electrochemical impedance spectroscopic (EIS) studies were performed in the frequency range between 100 mHz and 100 kHz using Electrochemical Impedance Analyzer PARC(EG&G) Model 6310. The excitation signal was 5mV. The analysis of the data was carried out using the computer programme written by Bouckamp and supplied by PARC(EG&G).

2.5. Maintenance of cell temperature

Measurements were carried out at several temperatures between ambient temperature and 80°C. For temperatures above the ambient temperature, the cell was heated with a heating tape using a temperature controller and a thermocouple. The temperature was controlled within $\pm$ 1°C of the set temperature. The cell was allowed for thermal equilibrium for about an hour before measurements. For studies related to the ageing, the cells were stored at ambient temperature as well as at 80°C continuously for several hundreds of hours. For the purpose of temperature-dependent studies, measurements were made at several temperatures up to 80°C.

2.6. Data quality - comparison with the literature

The EIS data of lithium-symmetrical cells, as represented in Nyquist form, contains a semicircle or a pair of semicircles depending on the composition of the polymer electrolyte film and cell temperature. This feature is qualitatively in agreement with the reported literature. Quantitative comparison of the present experimental results with the literature results was made by recording EIS at 80°C of a fresh lithium-symmetrical cell. The Nyquist plot is shown in Fig. 1. The interfacial resistance obtained is 80 Ω cm^2 which is in agreement with the reported values in literature[4]. Thus, the experimental conditions of cell fabrication and measurements are well comparable to the standards of reported literature.

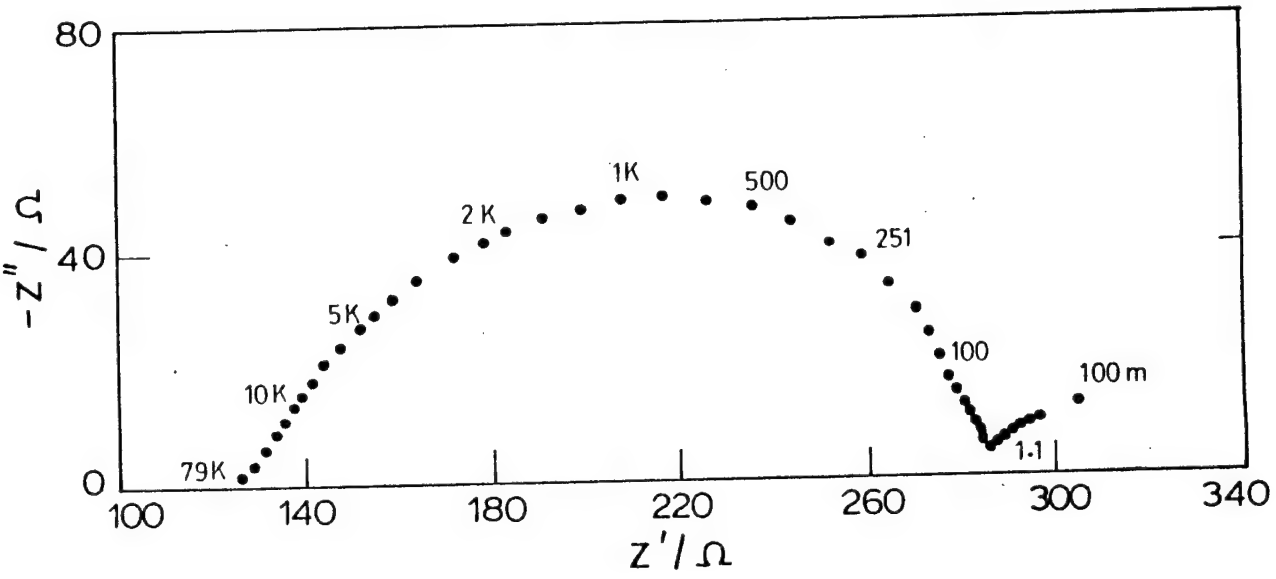

Figure 1. Nyquist plot of EIS data of freshly assembled $Li/PEO_8LiClO_4/Li$ cell at 80°C. Thickness of SPE = 125 μm and area of cross section = 1 cm^2. Frequency (Hz) at a few data points are shown.

3. RESULTS AND DISCUSSION

3.1. Ageing effect on Li/PEO_8LiClO_4/Li cells by galvanostatic voltage-transient method

In a symmetrical cell, the two lithium electrodes with their inherent surface films are separated by the SPE. As the two electrodes of the cell are identical, the open-circuit voltage of the cell is 0 V. At the instant of passing a galvanostatic current(I), there is a sudden rise in cell voltage followed by an exponential increase. A typical plot of the cell voltage transient is shown in Fig. 2. The equivalent circuit of the symmetrical cell is shown in Fig. 3.

Since the capacitors, C_{dl}, C_f and C_g attain complete charge in less than a second, the initial voltage rise (V_i) is attributed to the voltage drop across $[2(R_{ct}+R_f)+R_b]$. Therefore,

$$2(R_{ct}+R_f)+R_b = V_i / I \qquad (1)$$

or

$$2R_i+R_b = V_i / I \qquad (2)$$

where $R_i(=R_{ct}+R_f)$ is the interfacial resistance associated with the electron-transfer reaction and the surface film. If the resistance of SPE film (R_b) is known, the interfacial resistance (R_i) can be evaluated using Eqn. (2).

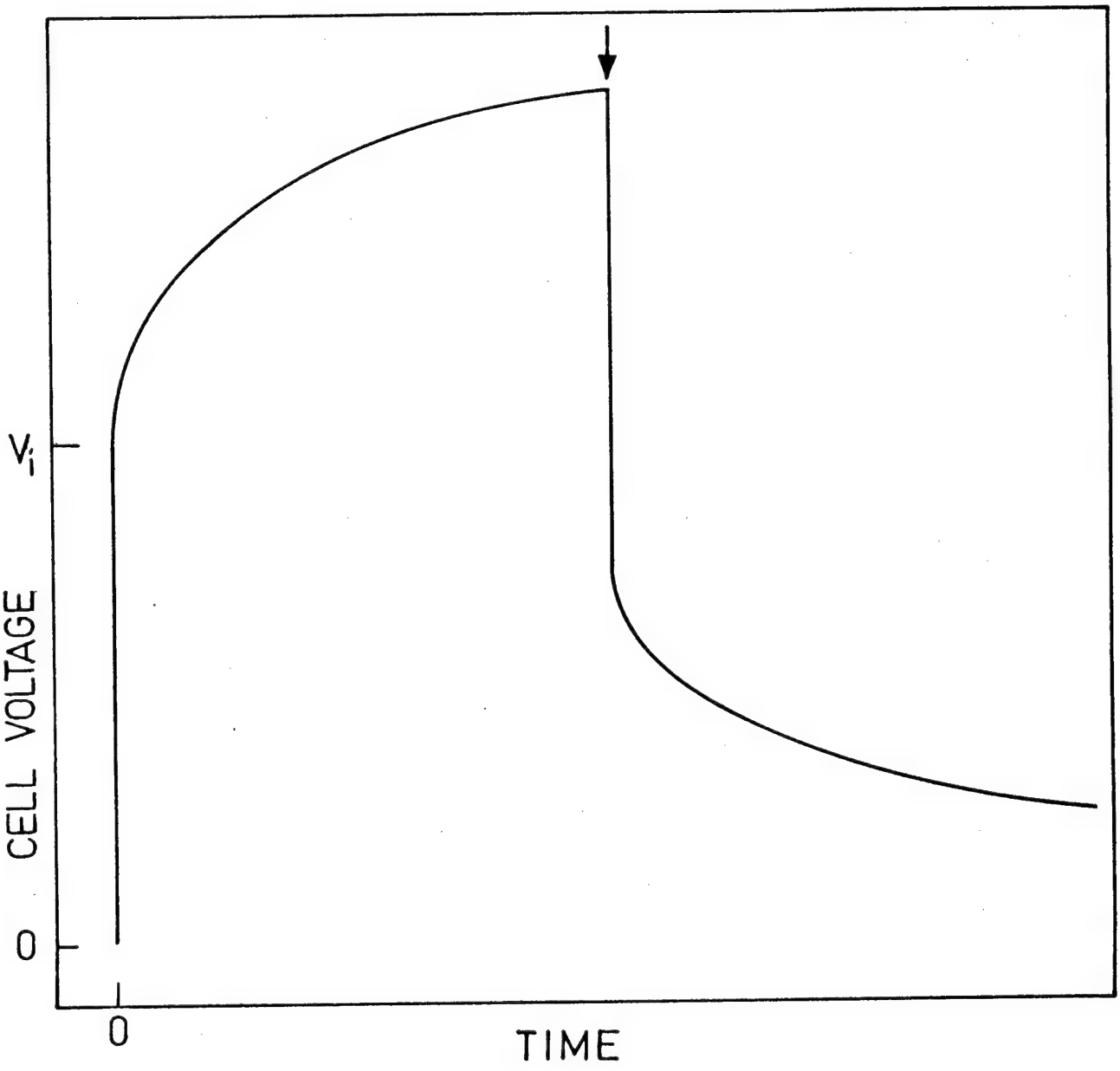

Figure 2. A schematic diagram of cell voltage as a function of time, when a d.c. current was passed through a $Li/PEO_8LiClO_4/Li$ cell. V_i is the initial voltage jump. Arrow indicates the time when the current was terminated.

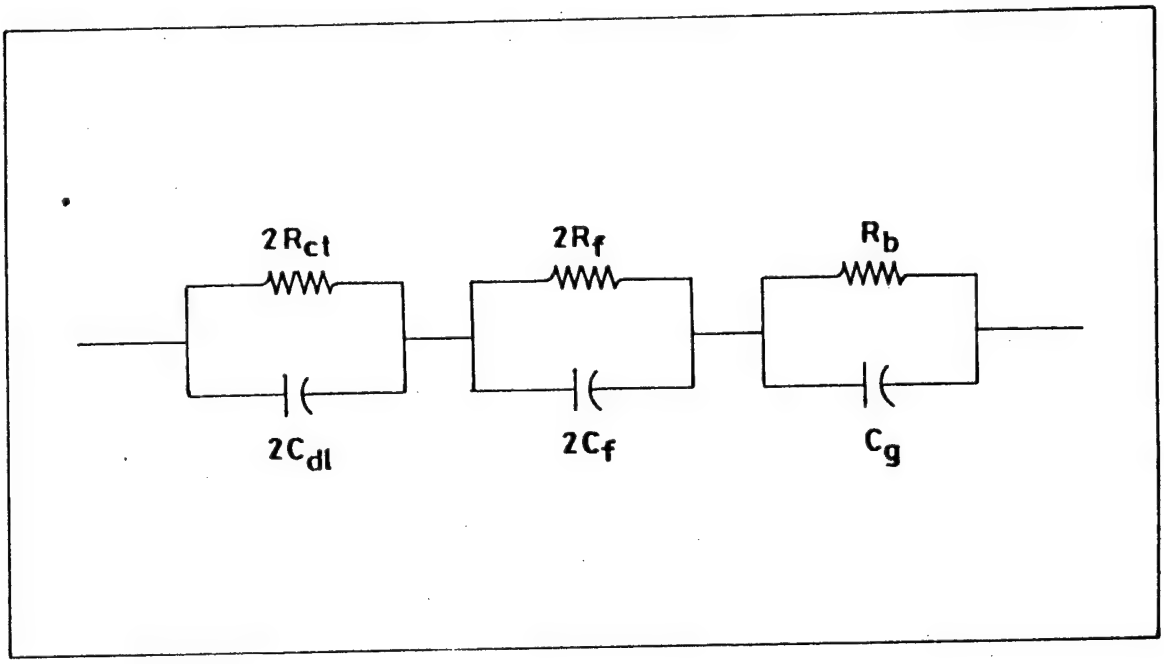

Figure 3. Equivalent circuit of a Li/PEO_8LiClO_4/Li symmetrical cell. R_{ct}, R_f and R_b are charge-transfer resistance at Li/passive layer, resistance of passive layer and resistance of SPE respectively. C_{dl}, C_f and C_g are double-layer capacitance at Li/passive layer interface, capacitance of passive layer and capacitance of polymer film respectively. R_{ct} of the two lithium electrodes are added and shown as 2 R_{ct}, so also R_f, C_{dl} and C_f.

The voltage transients of a symmetrical cell for different currents are shown in Fig. 4. The curves are reproduced by reversing the direction of current. The cell voltage at 15th s after current was allowed to pass was taken as V_i. The plots of V_i vs. I for several intervals of ageing are shown in Fig. 5. The plots are fairly linear. The slope (dV_i/dI) provides the sum of interfacial resistance and the resistance due to SPE, i.e., $2R_i+R_b$, in accordance with Eqn. (2). Using specific conductivity of PEO_8LiClO_4, viz., 5×10^{-4} S cm^{-1}, the resistance R_b of the film of 100 μm thickness and 1 cm^2 area of cross section is found to be 20 Ω at 80°C. Thus R_i was calculated using Eqn. (2). Assuming R_b to be invariant on ageing, the time evolution of R_i is shown in Fig. 6. The interfacial resistance of lithium in PEO_8LiClO_4 solid-polymer electrolyte increases with time after the cell is assembled. This increase is essentially attributed to the increase of resistance of surface film on lithium. It is believed that the surface film consists of two types of layers The immediate layer on lithium surface is known as primary passive film and is beneficial for the stability of the metal. When current flows through the electrode, the primary film allows Li^+ ions to diffuse through it without hindering electrochemical reaction. The secondary passive layer, which overlays the primary layer, is likely to hinder the passage of Li^+ ions through it. The increase in R_i (Fig. 6) is attributed to the secondary film due to increase in its thickness or the increase in the surface coverage, or the change in its chemical composition. The factors that may influence the passive film may include: (i) corrosion of

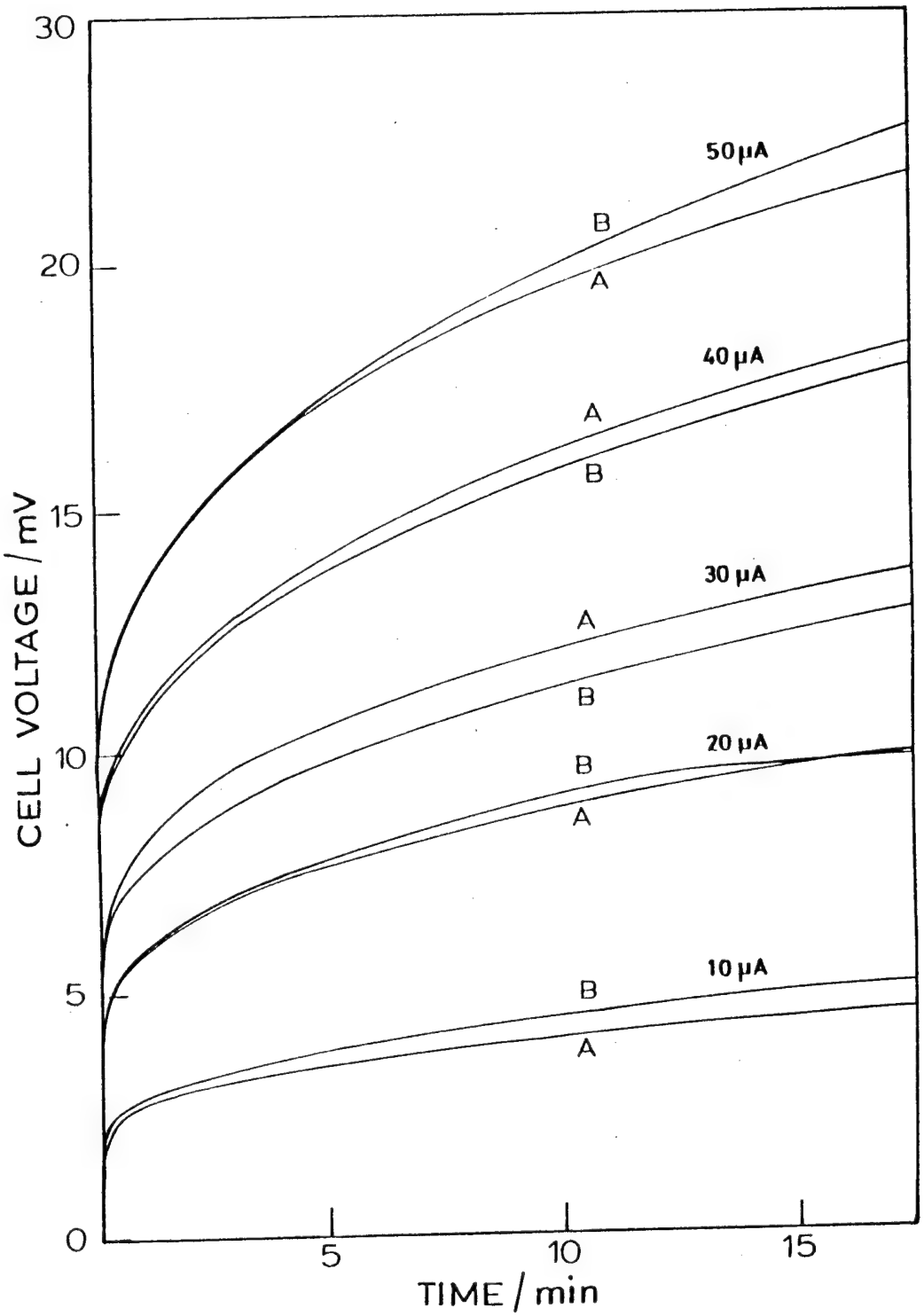

Figure 4. Voltage transients of $Li/PEO_8LiClO_4/Li$ symmetrical cell at different currents. A and B refer to forward and reverse directions of current respectively. Experiments was carried out 46 days after the cell was assembled. Cell temperature = 80°C, electrode area = 1.0 cm^2, and polymer electrolyte thickness = 100 μm.

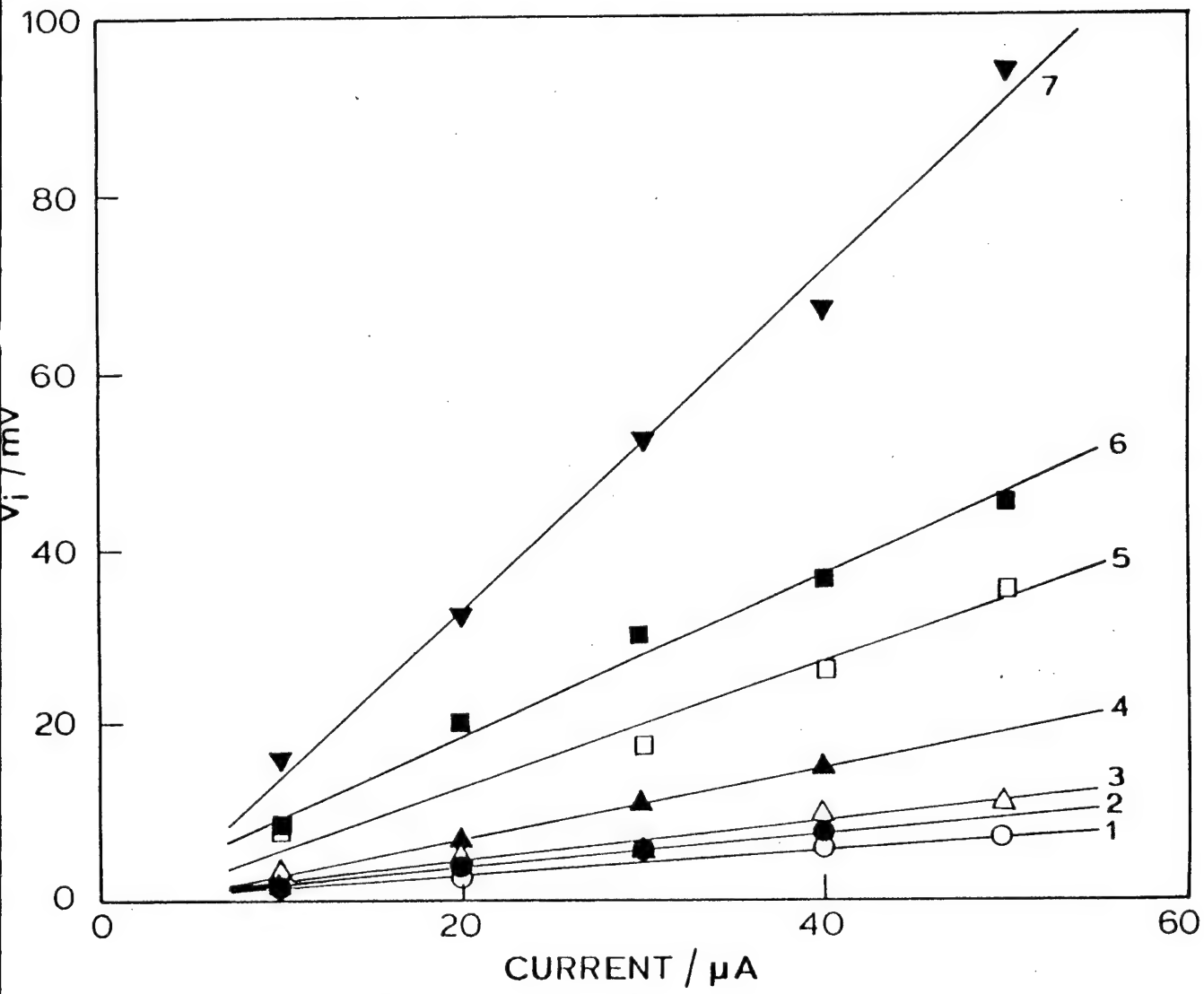

Figure 5. The initial voltage jump, V_i as a function of current flowing through the symmetrical cell when the ageing time was (1) 6, (2) 46, (3) 57, (4) 76, (5) 105, (6) 135 and (7) 165 days. Cell temperature = 80°C, electrode area = 1.0 cm^2, and polymer electrolyte thickness : 100 μm.

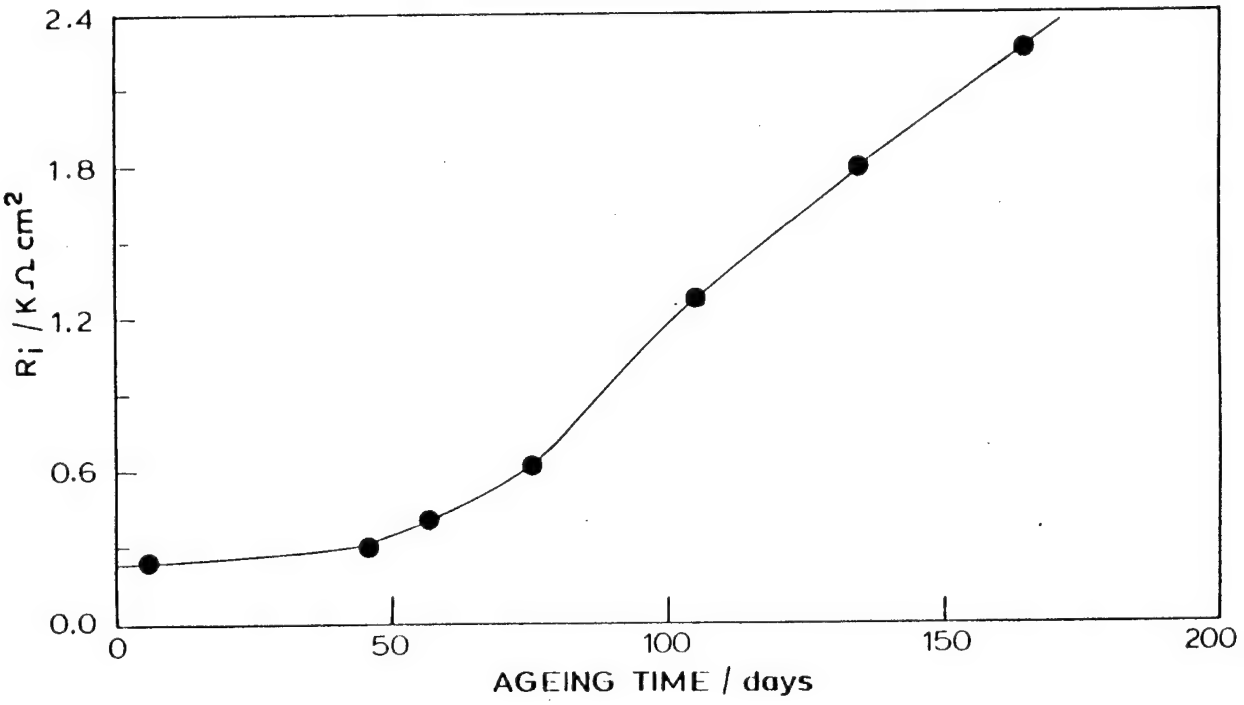

Figure 6. Time evolution of the interfacial resistance (R_i) of lithium in PEO_8LiClO_4 electrolyte at 80°C.

lithium during open-circuit conditions of cell; (ii) residual water present in SPE film; (iii) frequent heating of the cell to 80°C during experiments; and (iv) cycling of the cell by passing currents in the range 10 to 50 μA.

The exponential increase of cell voltage due to current flow (Fig. 4) can be attributed to slow diffusion of Li^+ ions in the surface passive film as discussed below.

The generally accepted electron transfer reaction at a lithium electrode is,

$$Li^+ + e^- = Li \qquad (3)$$

The equilibrium voltage (V_e) of the cell is given by,

$$V_e = E_e^c - E_e^a \qquad (4)$$

where E_e^c and E_e^a are equilibrium potentials of cathode and anode respectively. $V_e = 0$, as the cell under consideration is Li/SPE/Li. When current flows through the cell, the forward reaction occurs at the lithium cathode while the reverse reaction occurs at the anode. Lithium ions produced at the anode Li/surface film interface travel successively through the anode surface film, the solid-polymer electrolyte and the cathode surface film before reaching the cathode Li/surface film interface. Reduction of Li^+ ions occurs at the cathode Li/surface film interface and result in surface deposition. The transport of Li^+ ions in the surface film is considered to be

slower than the remaining steps. Hence, the concentration of Li^+ ions at the cathode/film interface is smaller than that in SPE and, simultaneously it is higher at the anode Li/film interface. The concentration gradients in the SPE are neglected.

The cell voltage (V_t) in the region of voltage increase is given by,

$$V_t = E_t^c - E_t^a + 2IR_f + IR_b \quad (5)$$

The cell overvoltage, $\Delta V_t (= V_t - V_e)$ is thus:

$$\Delta V_t = V_t = |\eta_t^c| + |\eta_t^a| + 2IR_f + IR_b \quad (6)$$

The variation of V_t is due to variations in overpotentials, $\eta_t^c (= E_t^c - E_e)$ and $\eta_t^a (= E_t^a - E_e)$ with time, which in turn depend on the variation of concentration of Li^+ ions at electrode/surface-film interface. Using the Nernst equation,

$$|\eta_t^c| = (RT/F) \ln[C_e/C_t^c] \quad (7)$$

and

$$|\eta_t^a| = (RT/F) \ln[C_t^a/C_e] \quad (8)$$

where C_e is the concentration of Li^+ ions in SPE. Eqns. (7) and (8) are justified considering the fact that reaction (3) is fast and reversible with the exchange current of about 10 mA cm^{-2}. Therefore, the electrode reactions do not occur under charge-transfer control when currents are small in magnitude as in the present study. At any instant t, the concentration decrease ($\ln C_e - \ln C_t^c$) at the

cathode/film interface is equal in magnitude to the concentration increase ($\ln C_t^a$ - $\ln C_e$) at the anode/film interface. Therefore:

$$|\eta_t^c| = |\eta_t^c| = \eta_t \tag{9}$$

Eqns. (6) and (9) yield:

$$V_t = 2\eta_t + 2IR_f + IR_b \tag{10}$$

On differentiation, Eqn. (10) becomes:

$$dV_t/dt = 2(d\eta_t/dt) \tag{11}$$

The time-dependence of concentration of Li^+ ions at the cathode/film interface may be obtained by differentiating Eqn. (7) with respect to time (t) as given below. Eqn. (7) is re-written as:

$$C_t^c / C_e = \exp(-\eta_t^c F/RT) \tag{12}$$

On differentiation Eqn. (12) yields:

$$(1 / C_e)(dC_t^c/dt) = - \exp(-\eta_t^c F/RT)(F/RT)(d\eta_t/dt) \tag{13}$$

or

$$dC_t^c/dt = -(FC_e/RT)(d\eta_t^c/dt)\exp(-\eta_t^c F/RT) \tag{14}$$

As the concentration C_t^c is governed by diffusion of Li^+ ions in the surface film when a constant current (I) flows through the cell, C_t^c can be evaluated by solving Fick's law of diffusion. In analogy with diffusion of an electroactive ion in diffusion layer of electrode/electrolyte interface:

$$C_t^c = C_e - 2It^{1/2}K / FAD^{1/2}\pi^{1/2} \tag{15}$$

where K is a constant related to thickness of the surface film on lithium and other symbols have their usual meanings.

Differentiating Eqn. (15) gives:

$$dC_t^c/dt = -IK / FAD^{1/2}\pi^{1/2}t^{1/2} \quad (16)$$

From Eqns. (14) and (16),

$$d\eta_t^c/dt = (IRTK / F^2AC_eD^{1/2}\pi^{1/2}t^{1/2})\exp(\eta_t^cF/RT) \quad (17)$$

Similarly, it can be shown that,

$$d\eta_t^a/dt = (IRTK / F^2AC_eD^{1/2}\pi^{1/2}t^{1/2})\exp(\eta_t^aF/RT) \quad (18)$$

Therefore, generalizing Eqn. (17) and (18) for either cathode or anode,

$$d\eta_t^c/dt = (IRTK / F^2AC_eD^{1/2}\pi^{1/2}t^{1/2})\exp(\eta_tF/RT) \quad (19)$$

From Eqns. (11) and (19):

$$dV_t/dt = (2RTK / F^2AC_eD^{1/2}\pi^{1/2}t^{1/2})\exp(\eta_tF/RT) \quad (20)$$

Eqn. (20) can be verified by the following :

(i) At any instant t, the product $[(dV_t/dt)\exp(-\eta_tF/RT)]$ should increase linearly with I.

(ii) For any constant current, the product $[(dV_t/dt)\exp(-\eta_tF/RT)]$ should increase linearly with $t^{-1/2}$.

The experimental data obtained with several current values in the 10-50 μA range and over several intervals during ageing of the symmetrical cells were

analyzed to verify the validity of Eqn. (20). A typical plot of dV_t/dt versus t is shown in Fig. 7. As may be expected from V_t versus t data (Fig. 4), dV_t/dt decreases with time and finally becomes invariant within about 10 min. The value of overpotential (η_t) at each Li electrode is calculated as $(V_t - V_i)/2$, and the product $[(dV_t/dt)\exp(-\eta_t F/RT)]$ versus I at several times are plotted. A typical plot for the data obtained 46 days after cell assembly is shown in Fig. 8. All the plots are linear. Similarly, $[(dV_t/dt)\exp(-\eta_t F/RT)]$ versus $t^{-1/2}$ plots shown in Fig. 9 are also linear. Thus, the data agree with Eqn. (20), and confirm the exponential voltage increase of the symmetrical cell which is due to diffusion-limited mass transport in the passive film present on the lithium surface.

If diffusion-limited mass transport in SPE is considered to explain the exponential increase of cell voltage, the slope (dV_t/dt) is expected to be invariant with ageing. A plot of (dV_t/dt) versus ageing time is shown in Fig. 10 for 20 μA cell current at several t values of V-t curves. The increase in (dV_t/dt) with ageing suggests that the process of voltage increase in associated with a passive layer on lithium. This corroborates further the above discussion. It may, therefore, be concluded that the time-dependent voltage variation in symmetrical cells on passing a galvanostatic current is due to the diffusion-limited transport of Li^+ ions in the surface passive film on lithium electrodes. This work is published [5].

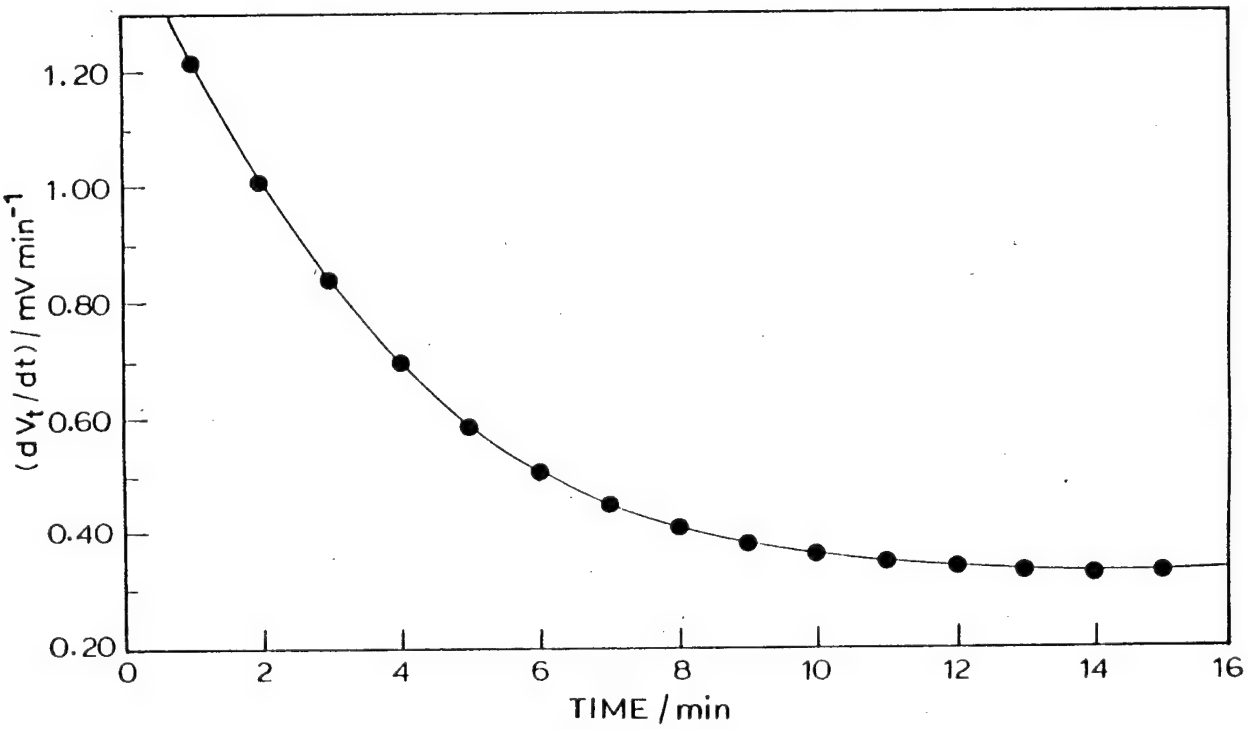

Figure 7. Variation of (dV_t/dt) with time of measurement at 50 μA. Experiment was carried out 6 days after cell assembly. Cell temperature = 80°C, electrode area = 1.0 cm^2 and polymer electrolyte thickness =100 μm.

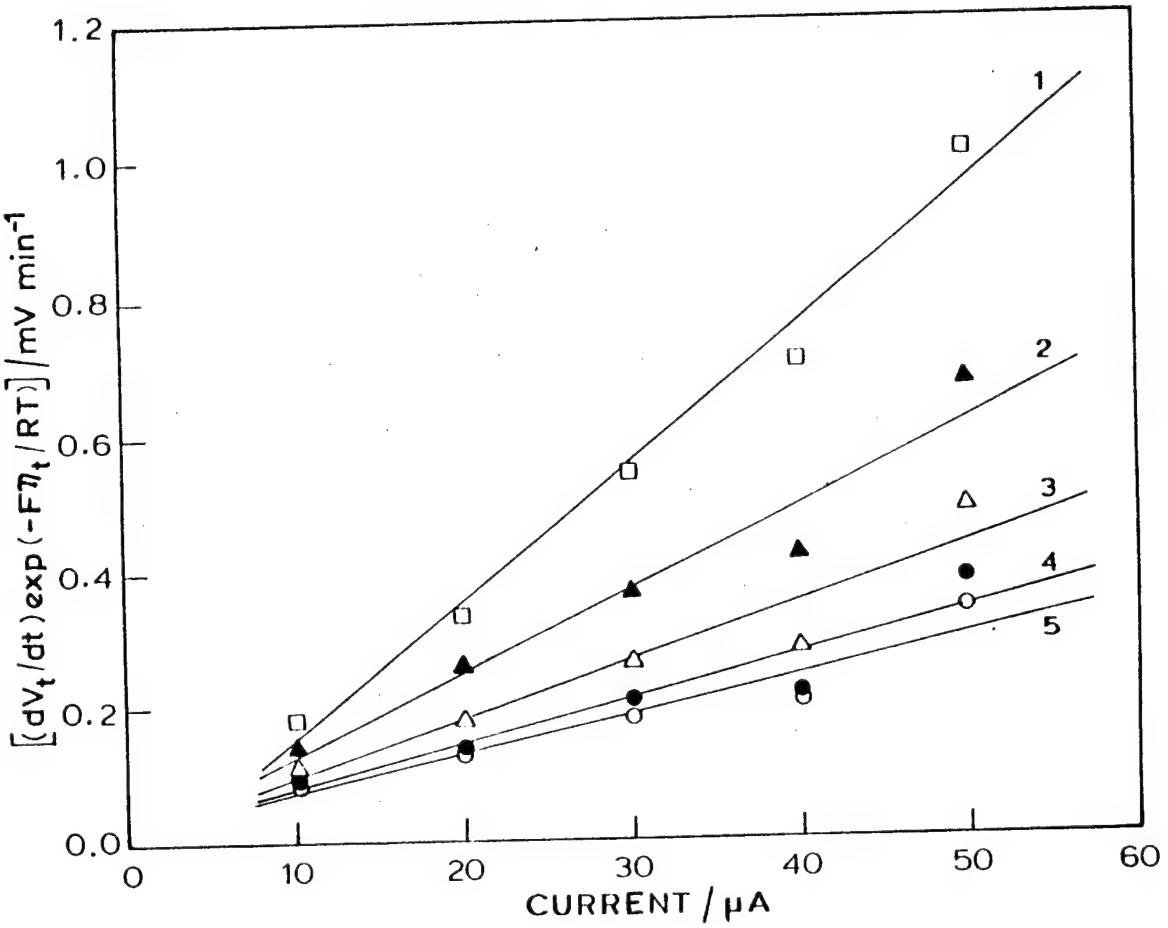

Figure 8. The product $[(dV_t/dt)\exp(-\eta_t F/RT)]$ as a function of current (I) when measured at (1) 2, (2) 4, (3) 6, (4) 8 and (5) 10 min during polarization. Experiment was carried out 46 days after the cell was assembled. Cell temperature = 80°C, electrode area = 1.0 cm^2 and polymer electrolyte thickness = 100 μm..

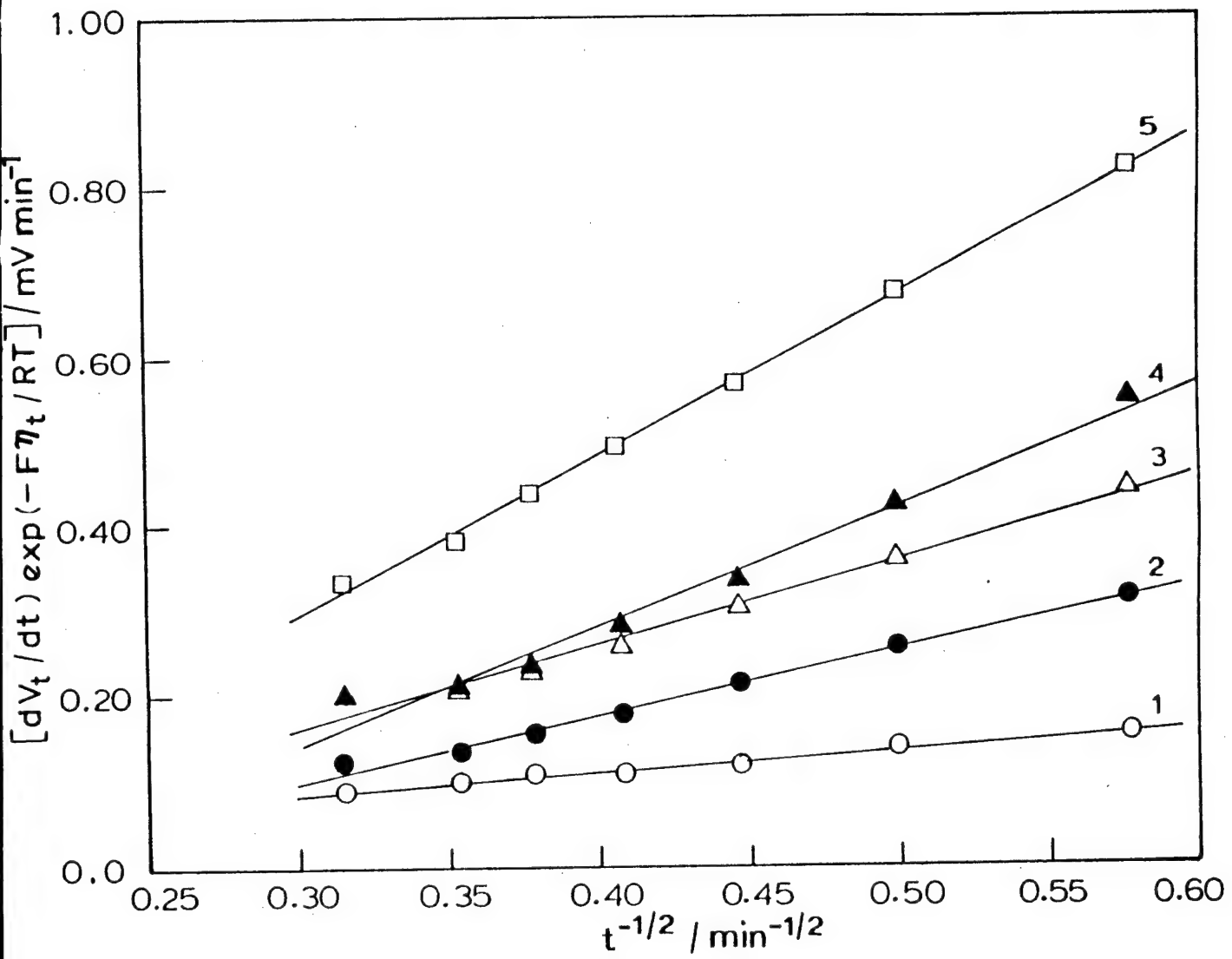

Figure 9. The product $[(dV_t/dt)\exp(-\eta_t F/RT)]$ as a function of $t^{-1/2}$ when the current was (1) 10, (2) 20, (3) 30 (4) 40 and (5) 50 μA. Experiment was carried out 46 days after the cell was assembled. Cell temperature = 80°C, electrode area = 1.0 cm^2 and polymer electrolyte thickness = 100 μm.

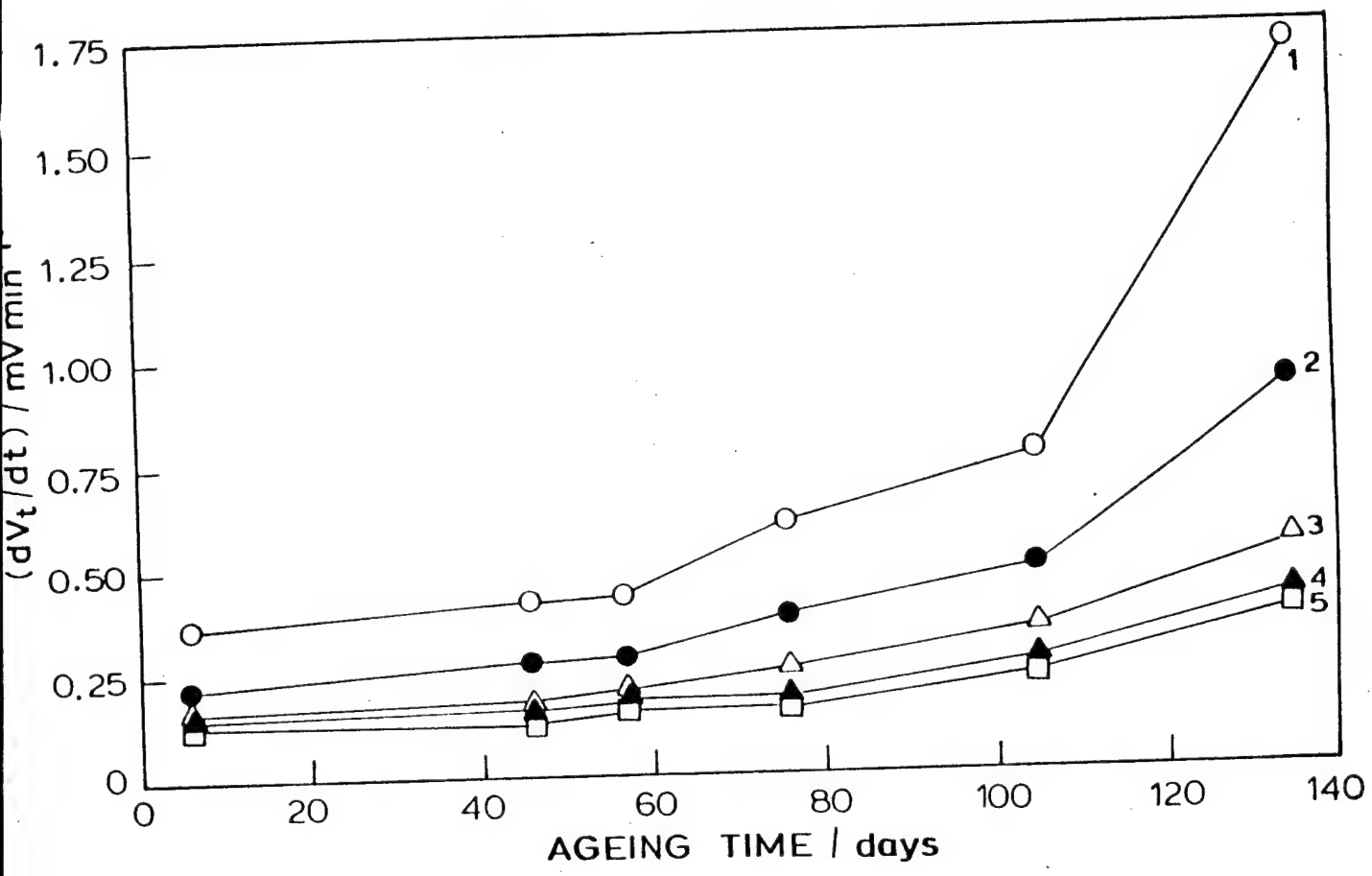

Figure 10. The slope, (dV_t/dt) as a function of ageing time when measured at (1) 2, (2) 4, (3) 6, (4) 8 and (5) 10 min during polarization. Cell temperature = 80°C, electrode area = 1.0 cm^2, polymer electrolyte thickness = 100 μm and galvanostatic current = 20 μA.

3.2. Data analysis of Electrochemical Impedance Spectroscopy

In literature, there is considerable ambiguity in the interpretation of EIS data of Li/electrolyte interface. While it is clear that the high frequency intercept of the Nyquist plot (Fig. 1) reflects the resistance of the electrolyte, the ambiguity is regarding the low frequency intercept, which is a measure of the interfacial resistance (R_i). While some authors [6] attribute R_i to the resistance (R_f) of the passive film on Li metal, others [7] consider it equal to the charge-transfer resistance (R_{ct}) of the reaction viz., $Li^+ + e^- = Li$ at metal/electrolyte interface. In the opinion of the author of this report, R_i reflects both the passive film resistance (R_f) and the charge-transfer resistance (R_{ct}), on the basis of the following arguments.

(i) In a recent publication, R_i is considered as the resistance of the passive layer on Li, based on a five-layer passive film model [6]. Although the values of R_i are reported in liquid electrolytes of different concentrations, the authors appear to have neglected to explain the concentration dependence. The concentration dependence can be explained in the following way if R_i is considered equal to R_{ct}.

The following charge-transfer reaction occurs at Li/electrolyte interface:

$$Li^+ + e^- = Li \quad (3)$$

The current potential characteristics of the reaction can be represented by Butler-Volmer equation.

$$I = I_o \ (e^{-\alpha F\eta/RT} - e^{(1-\alpha)F\eta/RT}) \quad (21)$$

where η is overpotential corresponding to current density (I), I_o is the exchange current density, α is the energy transfer coefficient and other symbols have their usual meanings. The exchange current density, I_o is related to the standard rate constant and concentration (C) of Li^+ ion according to the following relation [8]:

$$I_o = Fk^o C^{(1-\alpha)} \quad (22)$$

or, $$\ln I_o = \ln(Fk^o) + (1-\alpha)\ln C \quad (23)$$

On differentiation, we get

$$d\ln I_o/d\ln C = (1-\alpha) \quad (24)$$

Thus, a plot of $\ln I_o$ versus $\ln C$ is linear with a slope of $(1-\alpha)$. As the reaction (3) is reversible, the value of energy transfer coefficient α is expected about 0.5.

From the interfacial resistance (R_i) reported in Ref. [6] for different concentrations of $LiClO_4$ and $LiAsF_6$, I_o is calculated and is plotted as $\ln I_o$ versus $\ln C$. The plots are shown in Fig. 11. There is an increase of $\ln(I_o)$ with an increase of $\ln C$, although all the data points do not fall on a straight line. By

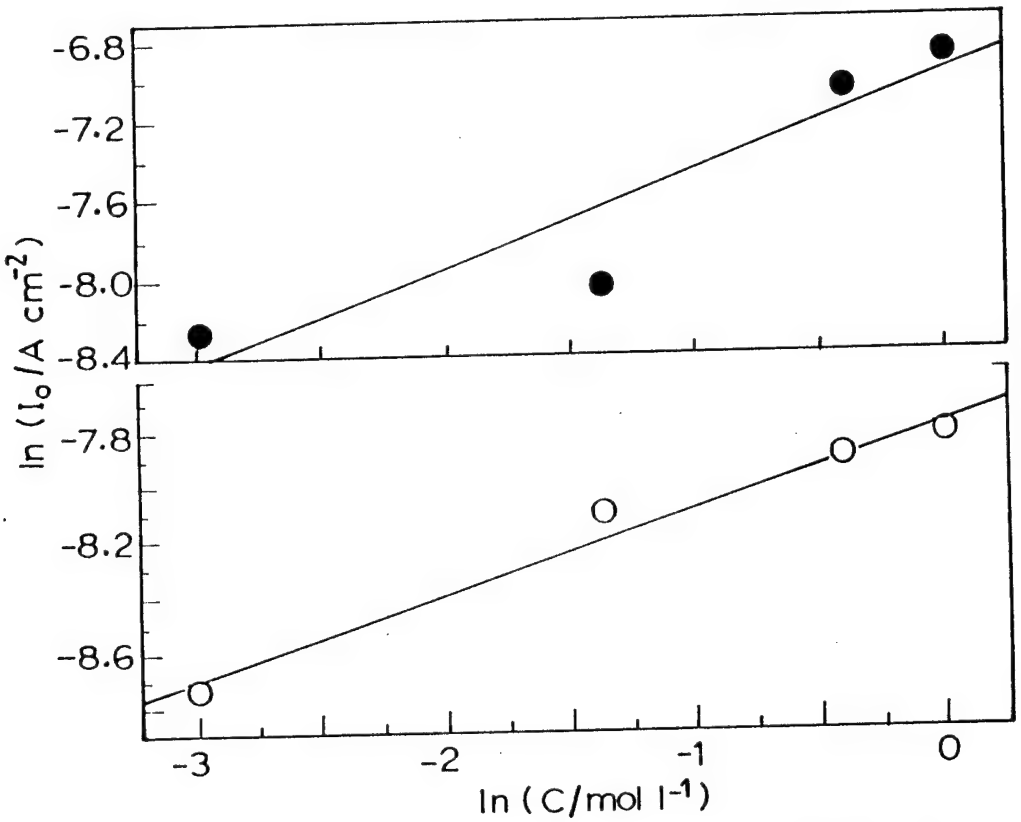

Figure 11. Exchange current density (I_o) as a function of concentration of lithium salt (C) for lithium electrode reaction in liquid electrolyte, (a) $LiClO_4$ and (b) $LiAsF_6$. (The values of I_o are calculated from resistance values reported in [6]).

drawing an average straight line fit, the slopes of the plots [=(1-α)] are obtained as 0.48 and 0.30. Thus, the energy-transfer coefficient, α is 0.52 and 0.70 for reaction (3) in $LiClO_4$ and $LiAsF_6$ solutions. The value of α in $LiClO_4$ solutions is close to 0.5 which is theoretically expected for reaction (3). However, α deviates to some extent in $LiAsF_6$. This analysis reveals that even though the authors of Ref. [6] have attributed the interfacial resistance (R_i) to the surface passive layer on Li, it appears that R_i more appropriately reflects the charge-transfer reaction.

(ii) The Nyquist plots of a Li symmetrical cell at two different ageing periods are shown in Fig. 12, for the purpose of comparison. The plot of the cell (Fig. 12(a)) within a few hours of its fabrication consists of a single semicircle, which is distorted to some extent. On ageing the cell at ambient temperature, the Nyquist plot (Fig. 12(b)) shows up an additional small semicircle at high frequency side (shown as A) and the bigger semicircle is distorted to a greater extent suggesting the presence of two semicircles (shown as B and C) overlapped in it. The appearance of semicircle A is due to the development of capacitive behaviour of the polymer electrolyte and to its decreased ionic conductivity. The semicircle B is attributed to parallel combination of resistance (R_f) and capacitance (C_f) of the passive film on lithium. The semicircle C is due to the parallel combination of the charge-transfer resistance (R_{ct}) of reaction (3) and double-layer capacitance (C_{dl}).

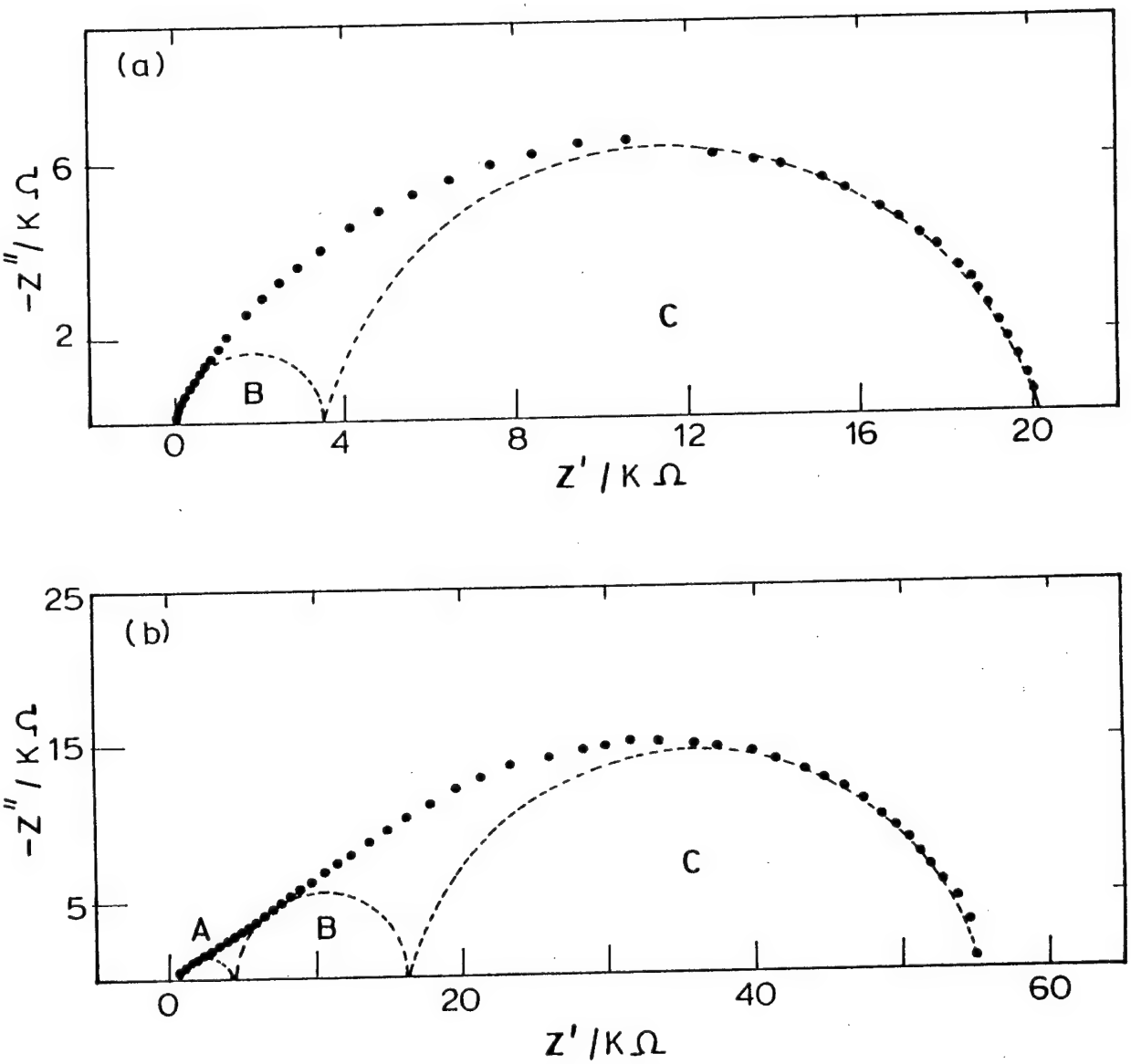

Figure 12. Nyquist plots of Li/PAN-PC-EC-$LiClO_4$/Li cell at a ageing time of (a) 70 h and (b) 925 h. The semicircle A is considered due to parallel combination of resistance and capacitance of the solid polymer electrolyte; the semicircle B is due to resistance and capacitance of the passive film on lithium metal; and semicircle C is due to the charge-transfer resistance and double-layer capacitance.

Thus, the data of Fig. 12(b) was analyzed using Bouckamp procedure based on the equivalent circuit shown in Fig. 13(a) and the resistance values were evaluated. When the SPE was highly conducting, the semicircle A was absent, e.g., in Fig. 12(a), and high frequency intercept of the Nyquist plot was not at the origin. In such case, the equivalent circuit shown in Fig. 13(b) was used for evaluating the values of resistances from Bouckamp fitting procedure.

For the purpose of fitting, constant phase elements were taken in place of capacitances as described in Ref [9]. The procedure involves initial estimation of the approximate values of resistances and constant phase elements. These values are used to evaluate refined values by nonlinear least square fitting procedure. The experimental data and the data generated using the evaluated circuit parameters agreed well (Fig. 14) and the χ^2 parameter was in the range of 10^{-4} to 10^{-5}.

3.3. Ageing of Li/PEO_8LiClO_4/Li and Li/PEO-PC-LiClO4/Li symmetrical cells at ambient temperature. EIS studies

Symmetrical cells of the type - (i) Li/PEO_8LiClO_4/Li, hereafter referred to as cell 1, and (ii) Li/PEO-PC-$LiClO_4$ (wt. ratio 1:1.33:0.13)/Li referred to as cell 2, were assembled and stored at ambient temperature for about 2000 h. The impedance spectra of the cells were periodically recorded during this period.

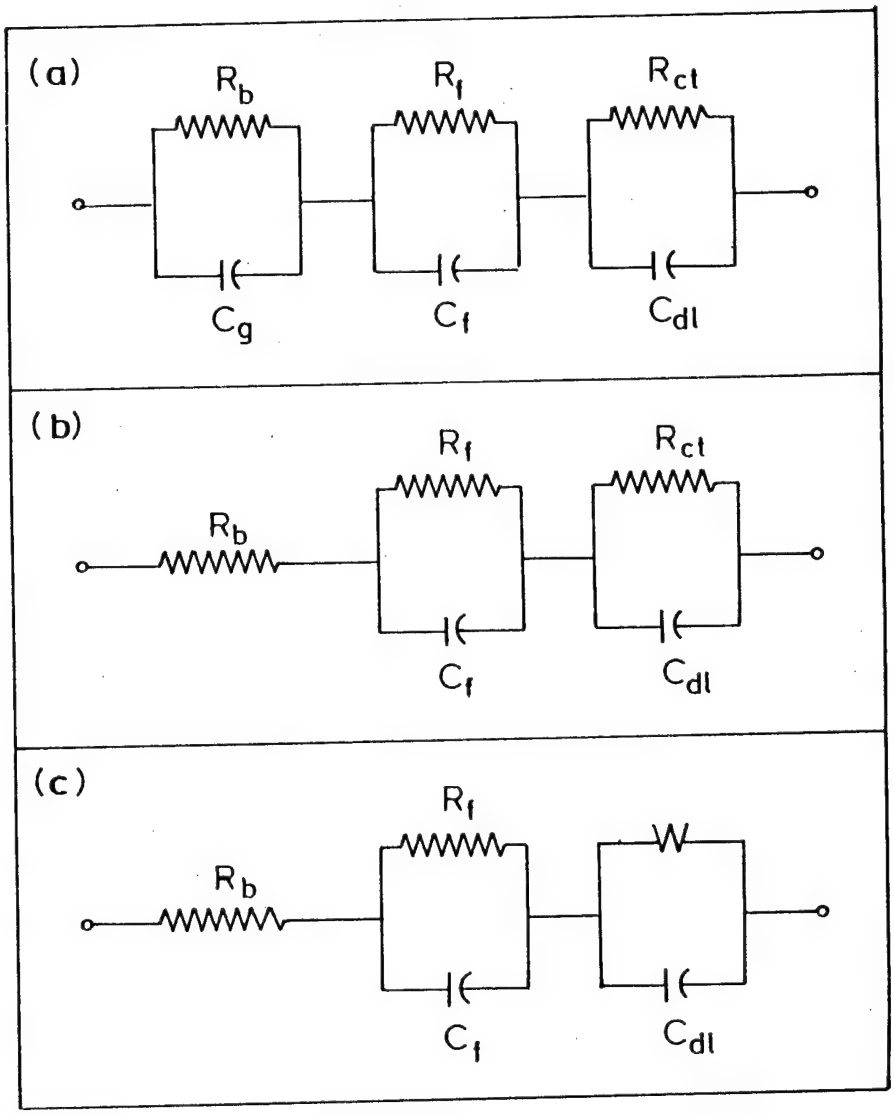

Figure 13. Equivalent circuits employed for evaluating R_b, R_f and R_{ct} from experimental impedance data by using Bouckamp equivalent circuit NLLS fit procedure. R_b, R_f and R_{ct} are resistances of polymer electrolyte film, surface passive film on Li and charge-transfer process respectively. C_g, C_f and C_{dl} are corresponding capacitances, and W is Warburg impedance. While doing fitting, capacitances were substituted by constant phase elements. One of the circuits was employed appropriate to the experimental data..

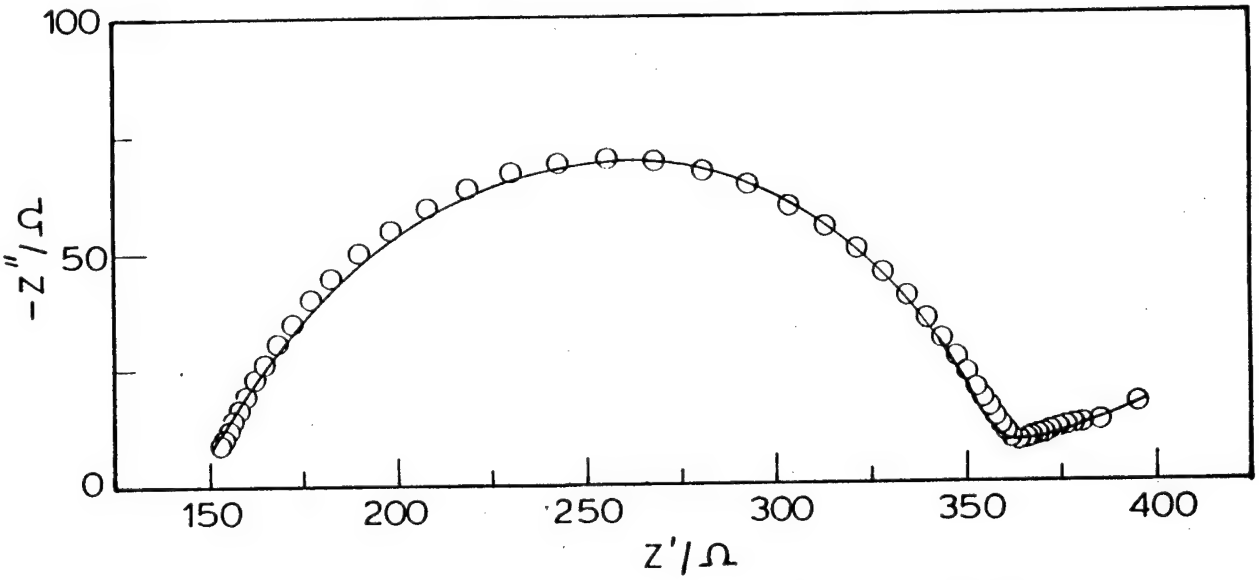

Figure 14. A typical Nyquist plot containing experimental data (-) and simulated data (o) from NLLS fitting procedure of Boukamp.

The Nyquist plot of the impedance spectrum recorded 48 h after Li/PEO_8LiClO_4/Li cell assembly is shown in Fig. 15 and the Bode plot in Fig. 16. Two semicircles are seen in Fig. 15. The appearance of high frequency semi-circle is only partial due to the frequency limit of the instrument being 100 kHz. The low frequency semicircle is distorted. This is attributed to overlap of two separate semi-circles, of which one semicircle corresponds to parallel R_f and C_f of passive film on Li and the other semicircle corresponds to parallel R_{ct} and C_{dl} of the interface, as discussed in Section 3.2. The EIS spectrum was analyzed using the equivalent circuit shown in Fig. 13(a), and the values of resistances R_b, R_f and R_{ct} were estimated. From the value of R_b specific conductivity (σ) of PEO_8LiClO_4 was obtained using the following eqn:

$$\sigma = l/R_bA \qquad (25)$$

where l is the thickness of polymer electrolyte film and A is its cross-sectional area. It was found that σ of PEO_8LiClO_4 film is 1×10^{-8} S cm^{-1} at 22°C. Similar values of σ for PEO_8LiClO_4 are reported in the literature. The resistance of the passive film on Li, i.e., R_f is obtained to be 17 kΩ cm^{-2} and R_{ct} is 40 kΩ cm^2.

Nyquist plots of Li/PEO_8LiClO_4/Li cell are shown in Fig. 17 for a few typical intervals of ambient temperature ageing. The values of R_b, R_f, R_{ct} and R_{cell} were evaluated from EIS data measured during ageing. Time evolution of

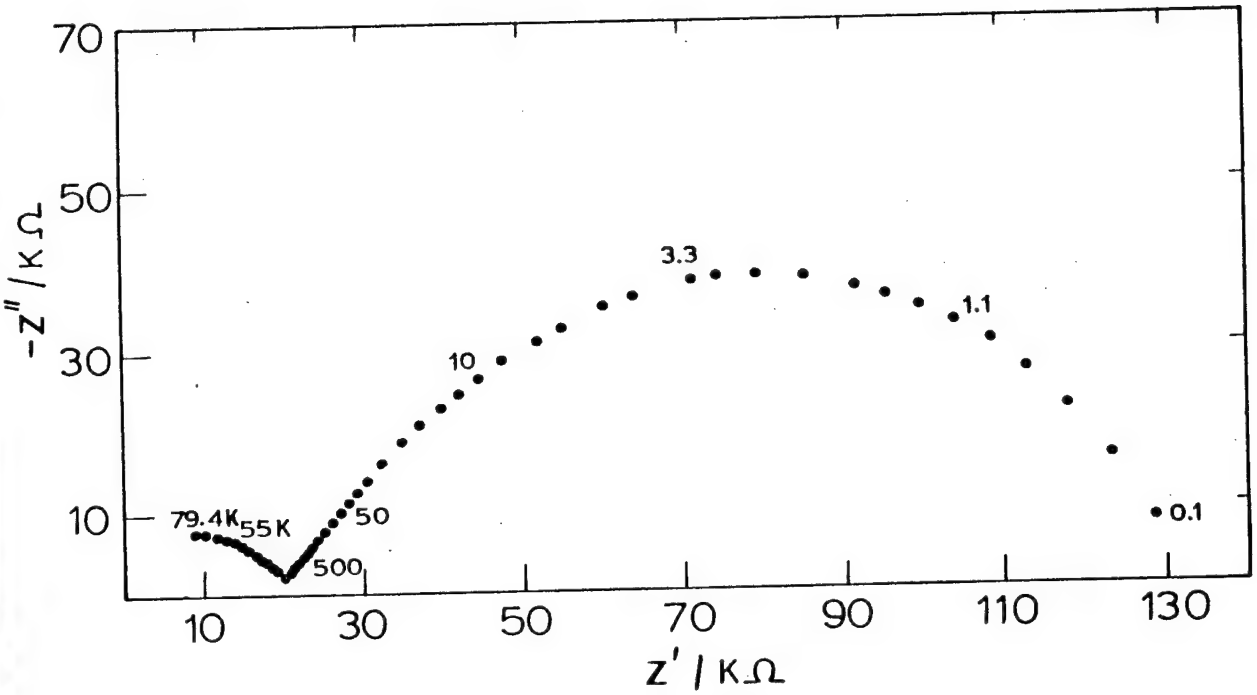

Figure 15 Nyquist plot of Li/PEO_8LiClO_4/Li cell at ambient temperature 48 h after the cell was assembled. Frequency (Hz) is shown at a few data points of the impedance spectrum.

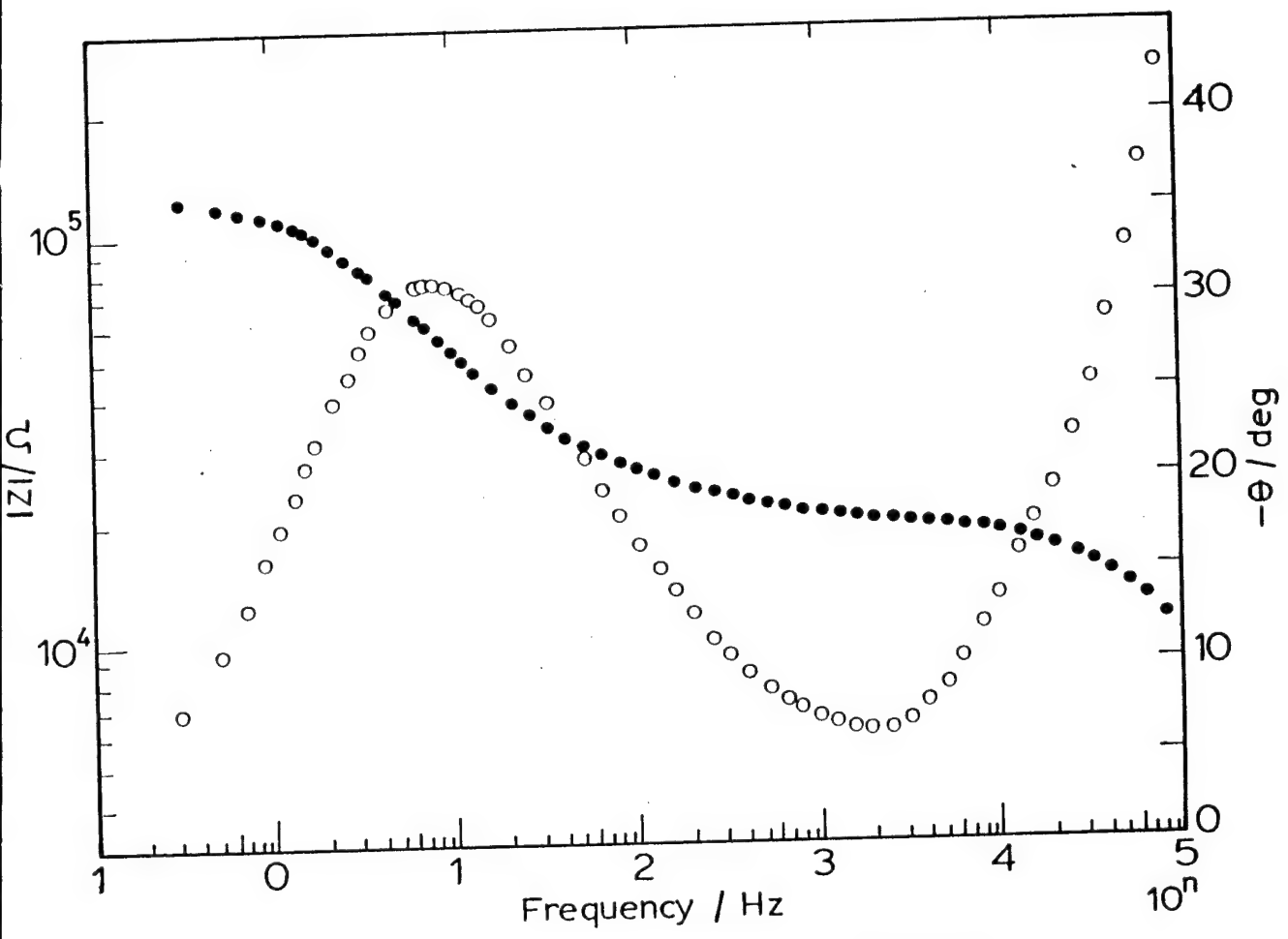

Figure 16. The EIS data of Figure 15 shown as Bode plot. The modulus of impedance (|Z|) is shown as ● and the phase angle (0) as O.

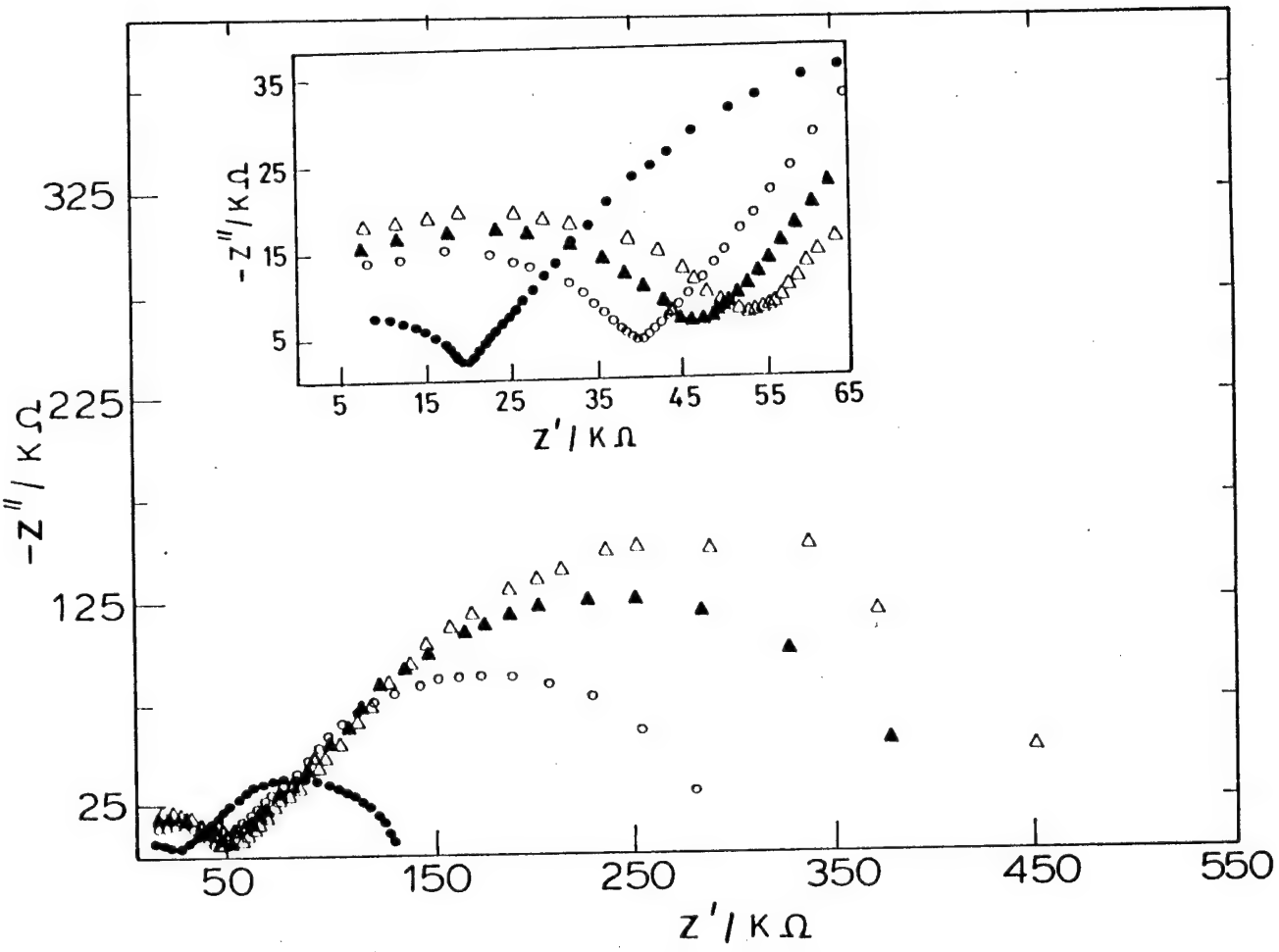

Figure 17. Nyquist plots of Li/PEO_8LiClO_4/Li cell at ambient temperature when the cell was aged for 48 h (●), 205 h(O), 520 h (▲) and 1020 h (Λ). An expanded portion of the plot near origin is shown as inset.

R_{cell}, R_f and R_{ct} during ageing of the cell is shown in Fig. 18. It is seen that the resistances steadily increase with ageing of the cell.

The Nyquist and Bode plots of the impedance spectrum recorded 48 h after Li/PEO-PC-$LiClO_4$/Li cell assembly are shown in Figs. 19 and 20 respectively. Outwardly, a semicircle is seen in the Nyquist plot (Fig. 19) which is, however, somewhat distorted. Following the arguments described in Section 3.2, the overlap of two semicircles is considered. The semicircle towards the high frequency zone is attributed to the parallel combination R_f and C_f of passive film on Li, whereas the semicircle at low frequency zone is due to parallel combination of R_{ct} and C_{dl} of the reaction at the Li/polymer electrolyte interface. The high frequency intercept of the semicircle is taken to be the ionic resistance (R_b) of the polymer electrolyte film. Nyquist plots of Li/PEO-PC-$LiClO_4$/Li cell are shown in Fig. 21 for a few typical intervals of ambient temperature ageing. Time evolution of R_{cell}, R_f and R_{ct} is shown in Fig. 22. As in the case of cell1, the values increase on ageing of the cell.

A comparative evaluation of cell1 and cell 2, which were aged at ambient temperature, is interesting. R_{cell} of the cells as a function of ageing time is shown in Fig. 23. The cell 2 has much lower resistance than the cell 1 in the

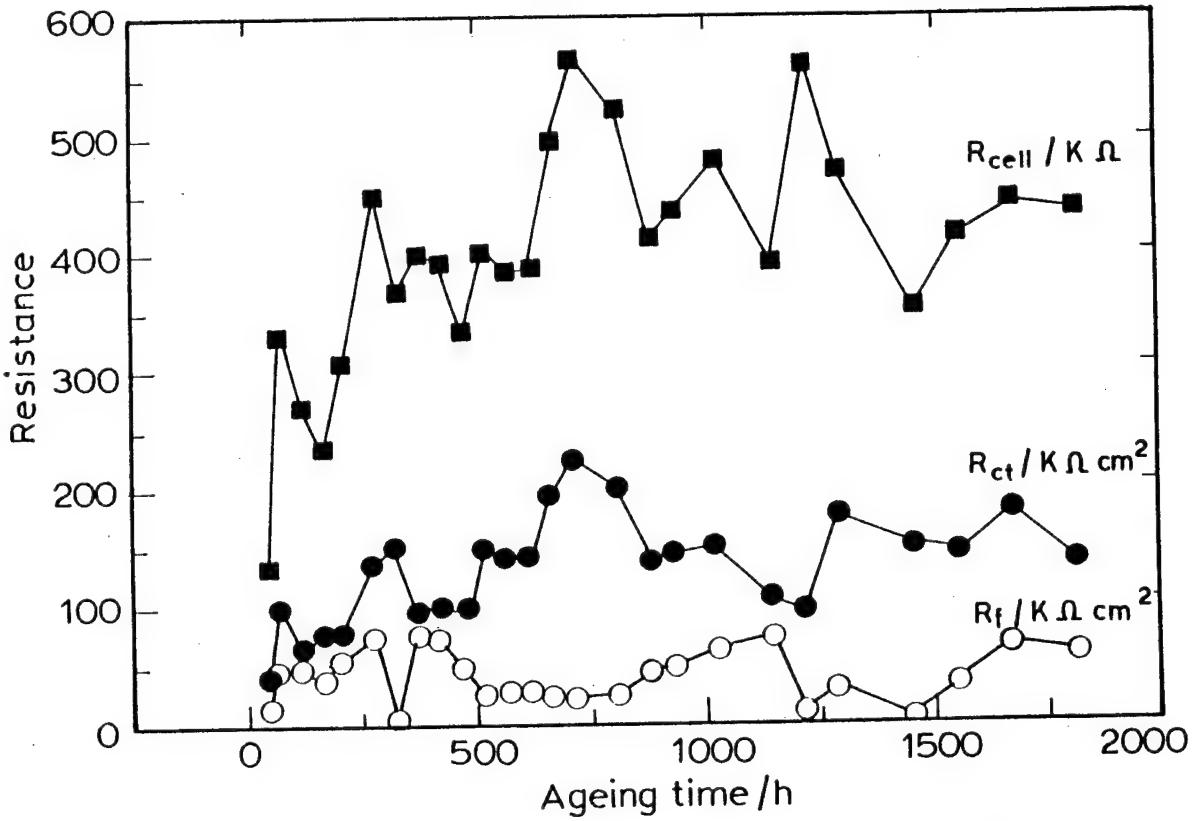

Figure 18. The cell resistance (R_{cell}), charge transfer resistance(R_{ct}) and passive film resistance (R_f) obtained from EIS data of Li/PEO_8LiClO_4/Li cell against ageing time at ambient temperature.

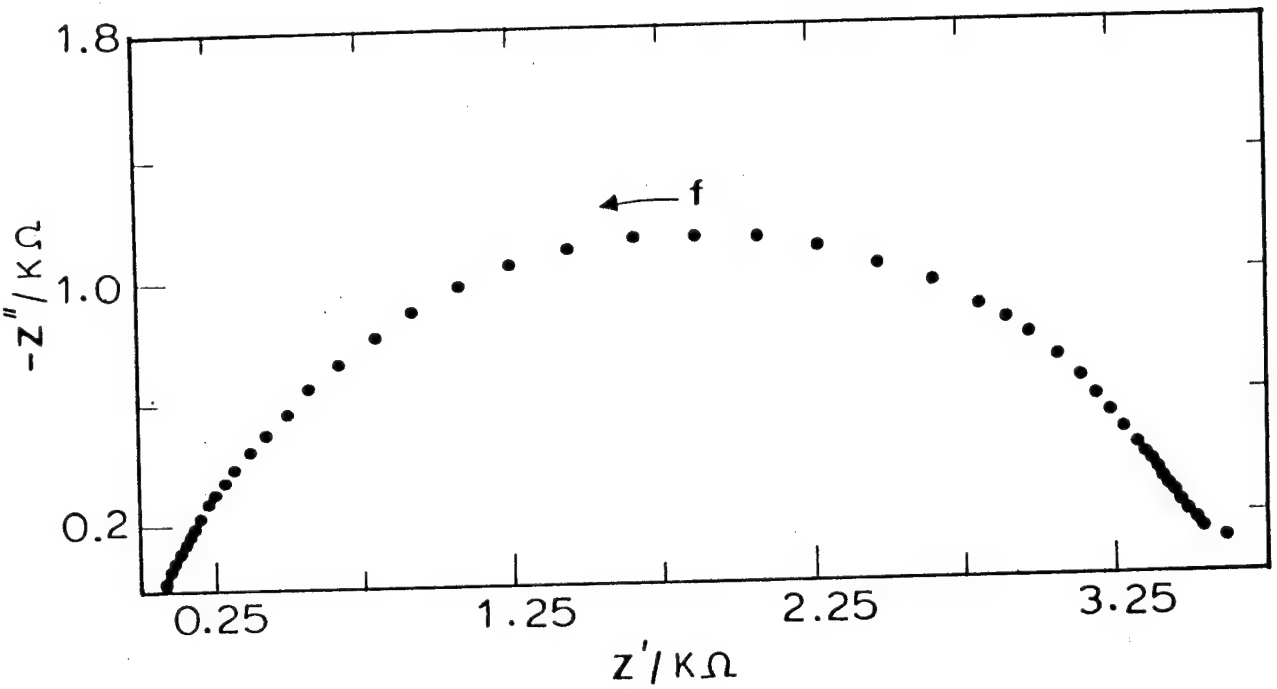

Figure 19. Nyquist plot of Li/PEO-PC-$LiClO_4$/Li cell at ambient temperature 48 h after the cell was assembled.

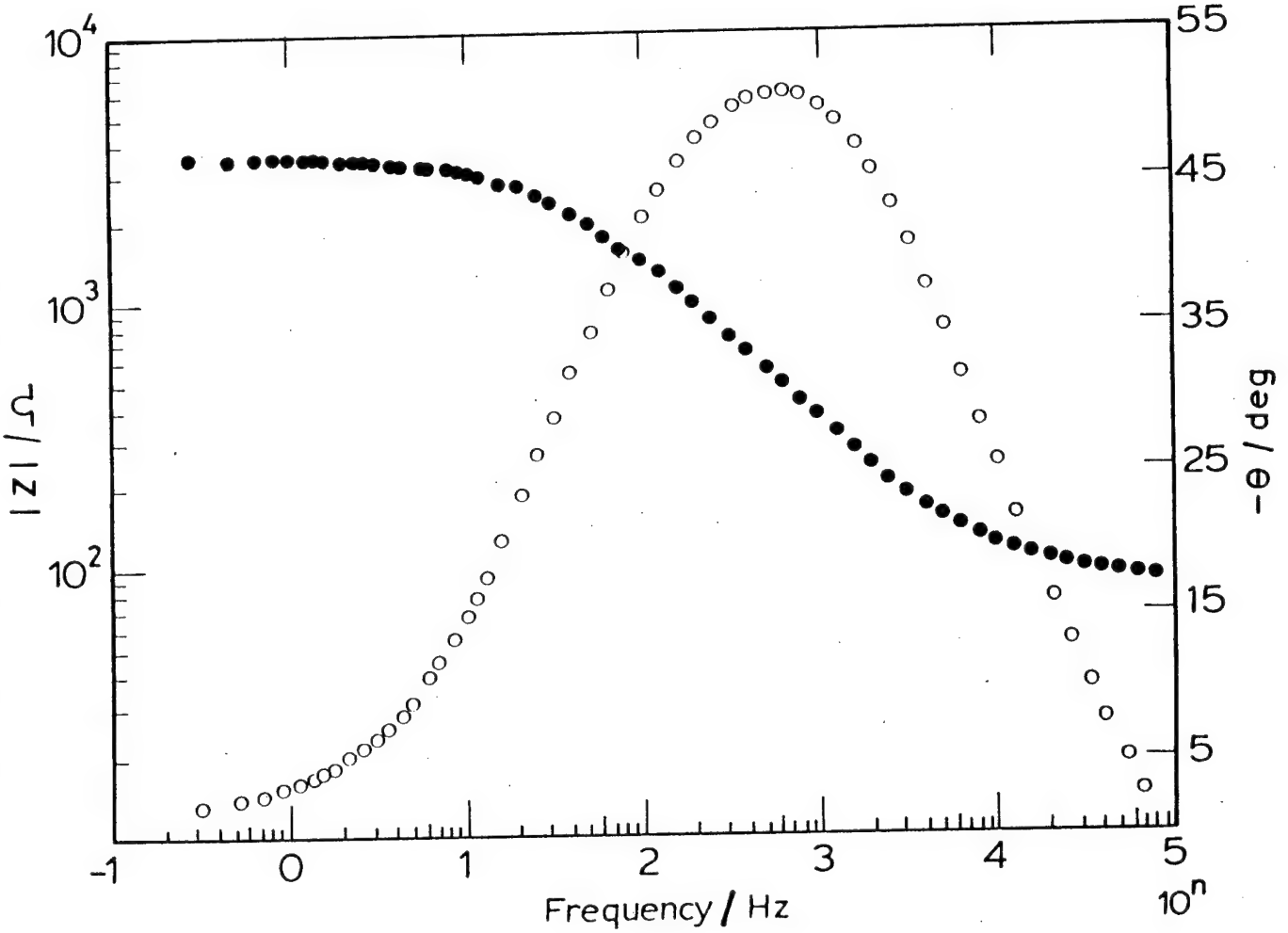

Figure 20. The EIS data of Figure 19 shown as Bode plot. The modulus of impedance (|Z|) is shown as ● and the phase angle (0) as O.

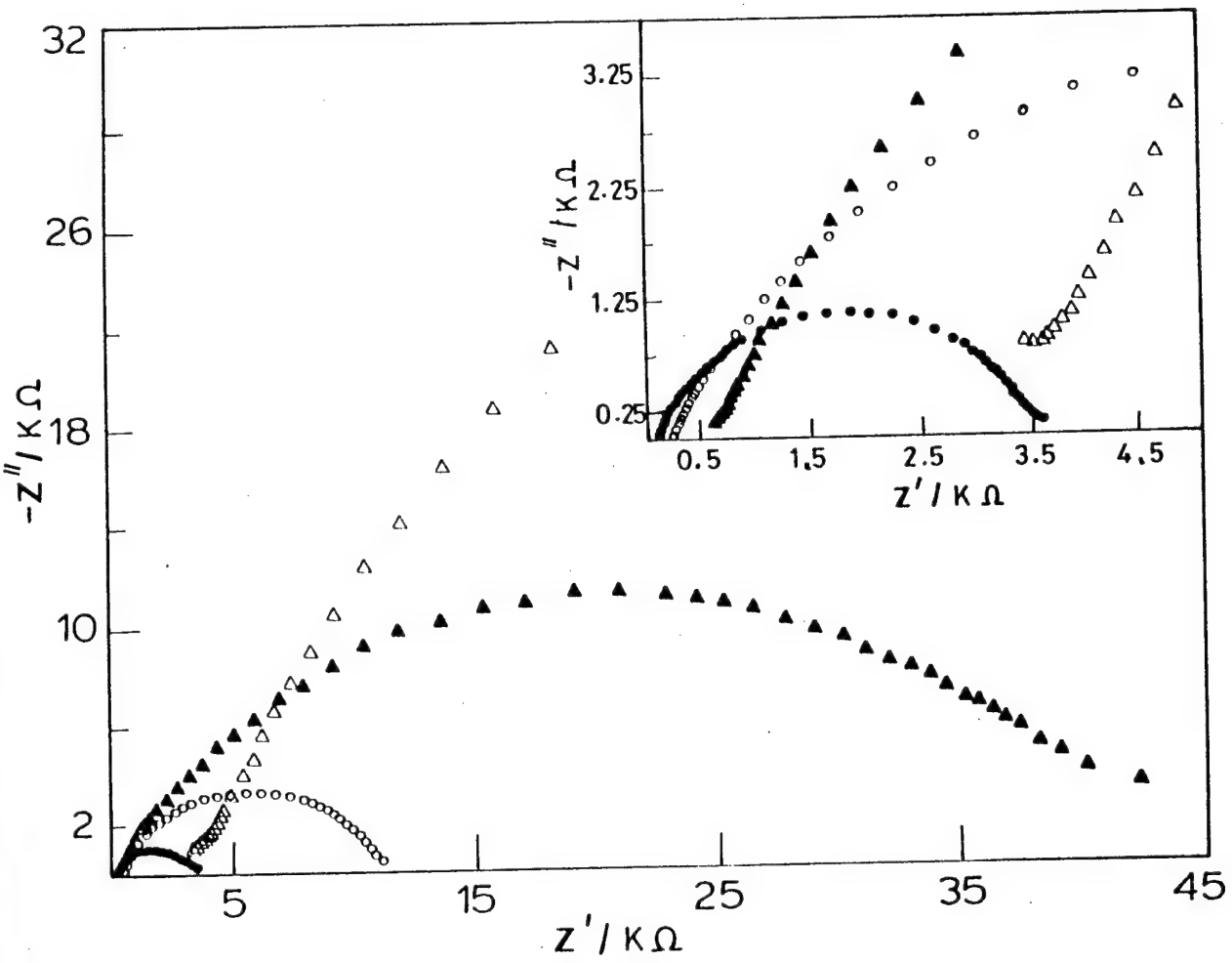

Figure 21. Nyquist plots of Li/PE-PC-$LiClO_4$/Li cell at ambient temperature when the cell was aged for 48 h(●), 205 h(O), 520 h (▲) and 1020 h (Δ). An expanded portion of the plot near origin is shown as inset.

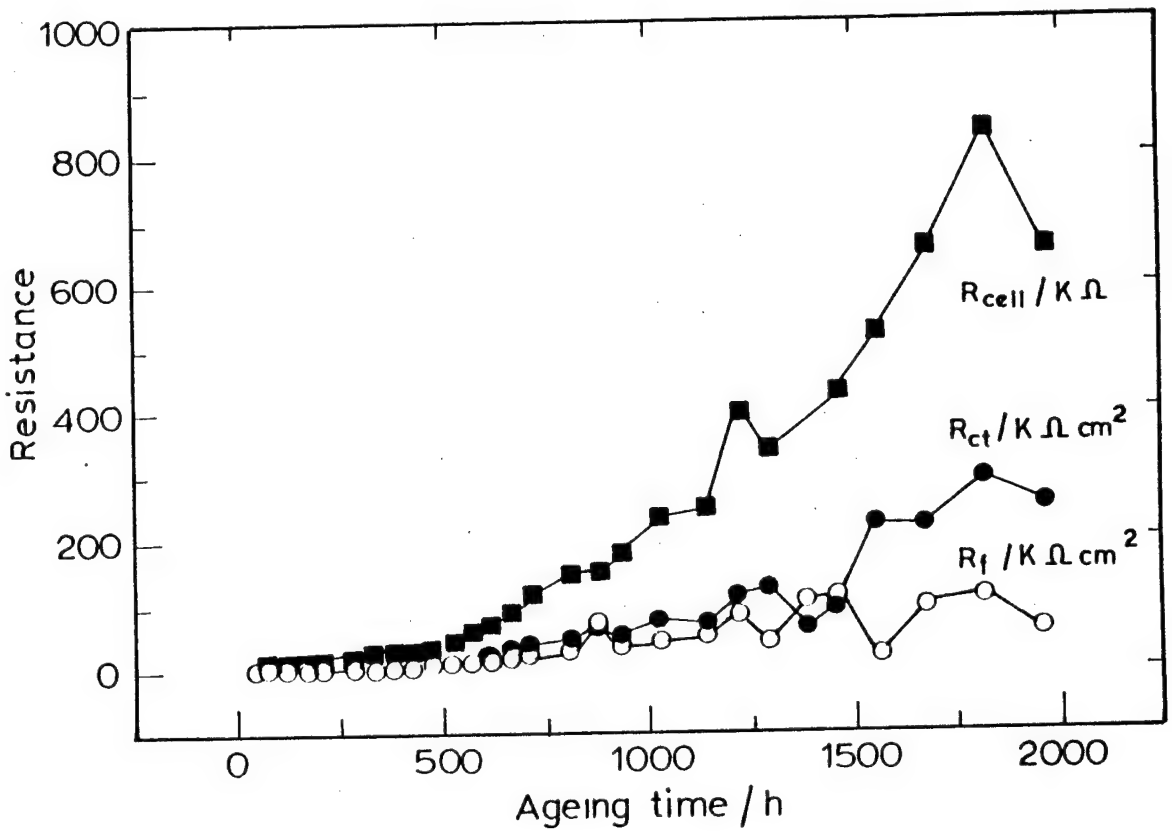

Figure 22. The cell resistance (R_{cell}), charge transfer resistance (R_{ct}) and passive film resistance (R_f) obtained from EIS data of Li/PEO-PC-$LiClO_4$/Li cell against ageing time at ambient temperature.

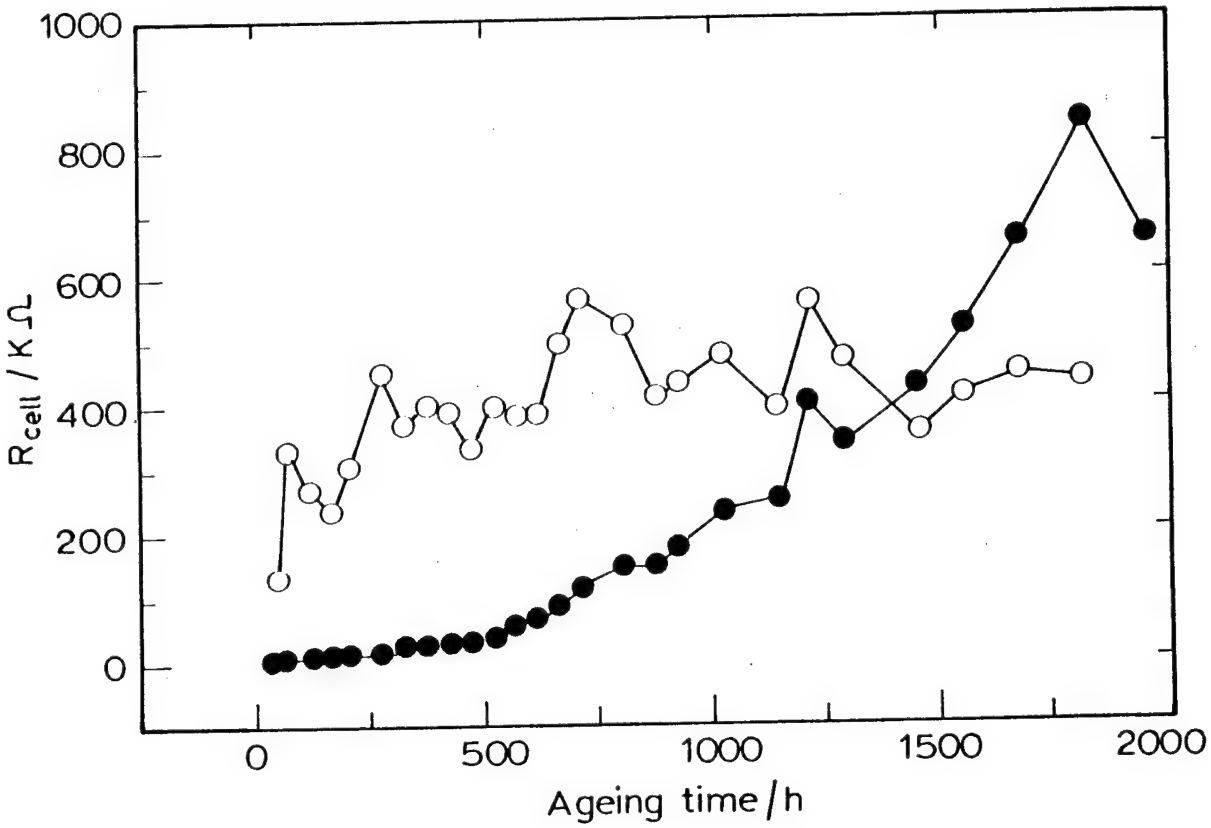

Figure 23. Cell resistance (R_{cell}) of Li/PEO_8LiClO_4/Li (O) and Li/PEO-PC-$LiClO_4$/Li (●) as a function of ageing time at ambient temperature.

initial stages of ageing. The lower resistance of cell 2 is due to higher conductivity of the SPE film. With an increase of storage time, R_{cell} of cell 2 increases steadily and becomes greater than R_{cell} of cell 1. It suggests that the beneficial effect of PC on conductivity decays gradually thus increasing the overall cell resistance. The increase in R_{cell} of cell 2 is reflected in a decrease of specific conductivity (σ) from 10^{-4} S cm^{-1} range down to 10^{-6} S cm^{-1} range (Fig. 24). The tendency of σ of PEO-PC-$LiClO_4$ to approach the σ of PEO_8LiClO_4 over a long period of ageing suggests that there is a gradual loss of PC from the electrolyte. The loss of PC can be attributed to a continuous corrosion of lithium metal at a faster rate than in the absence of PC. In a similar fashion, the I_o in PEO-PC-$LiClO_4$ at initial stages of ageing is at 10^{-5} A cm^{-2} range and it decreases to 10^{-7} A cm^{-2} range over a period of 2000 h (Fig. 25). Evidently, it is due to a rapid growth of passive film on Li in PEO-PC-$LiClO_4$.

It is estimated that the specific conductance of the passivating layer on lithium is about 1 x 10^{-9} S cm^{-1} at ambient temperature [10]. Using this value and the resistance (R_f) obtained in the present results, thickness (l) of the passivating layer is calculated following eqn. (25). Thus the value of l becomes 1650 Å in PEO_8LiClO_4 and 50 Å in PEO-PC-$LiClO_4$ when the symmetrical cells were fresh. The thickness of passive layer is shown as a function of ageing time in

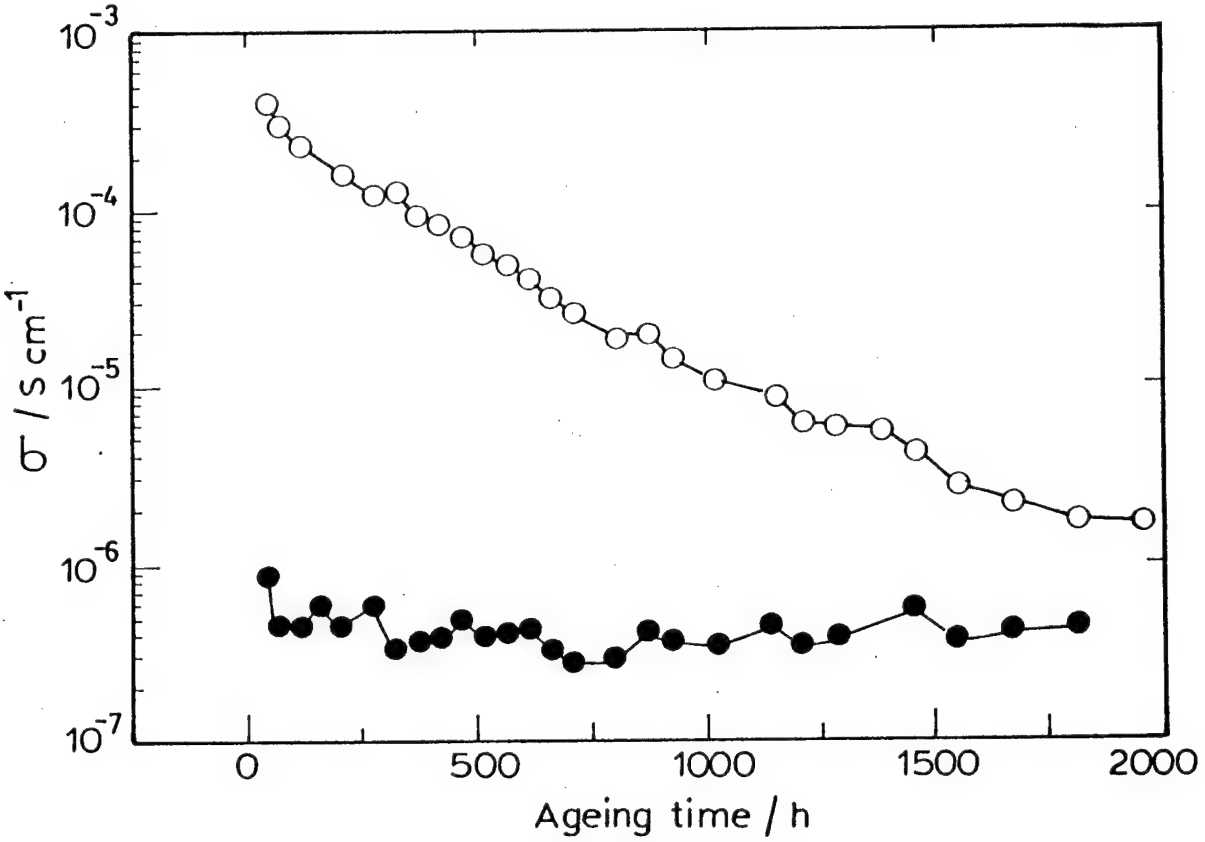

Figure 24. Specific conductivity (σ) of PEO_8LiClO_4 (●) and PEO-PC-$LiClO_4$ (O) as a function of ageing time at ambient temperature.

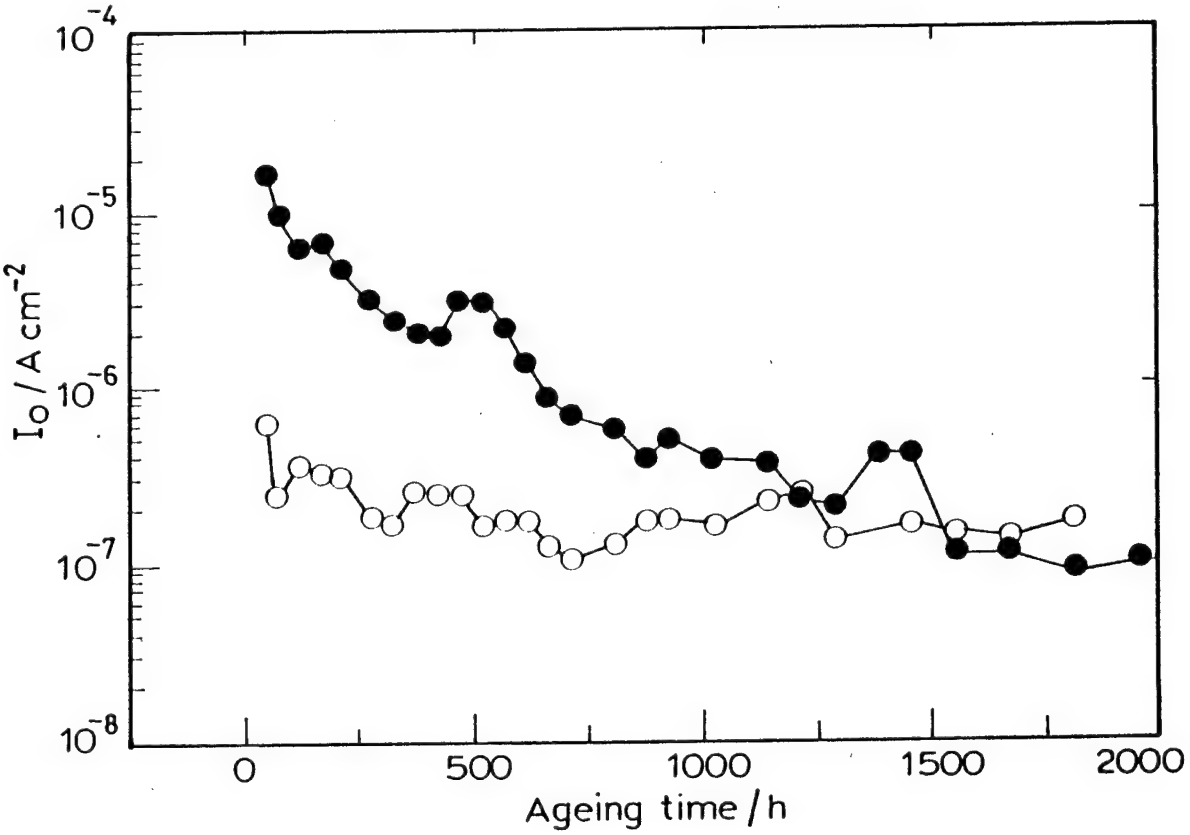

Figure 25. Variation of exchange current density (I_o) of $Li^+ + e^- = Li$ reaction in PEO_8LiClO_4(O) and PEO-PC-$LiClO_4$ (●) at ambient temperature.

Fig. 26. The value of l remains more or less invariant with an average value of 4500 Å on ageing in PEO_8LiClO_4, whereas it increases gradually in PEO-PC-$LiClO_4$ electrolyte.

It is clear that the thickness(l) of passivating layer on lithium in PEO-PC-$LiClO_4$ electrolyte is time dependent.

$$l = kt^n \qquad (26)$$

where k is proportionality constant and n is order of film formation. The above equation can be rewritten as:

$$\ln l = \ln k + n \ln t \qquad (27)$$

By differentiating w.r. to lnt, we get

$$d\ln l/d\ln t = n \qquad (28)$$

The value of n is obtained from the slope of lnl versus lnt plot (Fig. 27) and it is about 2.

3.4. Mechanism of passive film formation

It is evident from the results of ageing of the cells that the increase of passive-film resistance and decrease of specific conductivity of SPE take place simultaneously. A decrease in σ can be attributed to either an increase or decrease

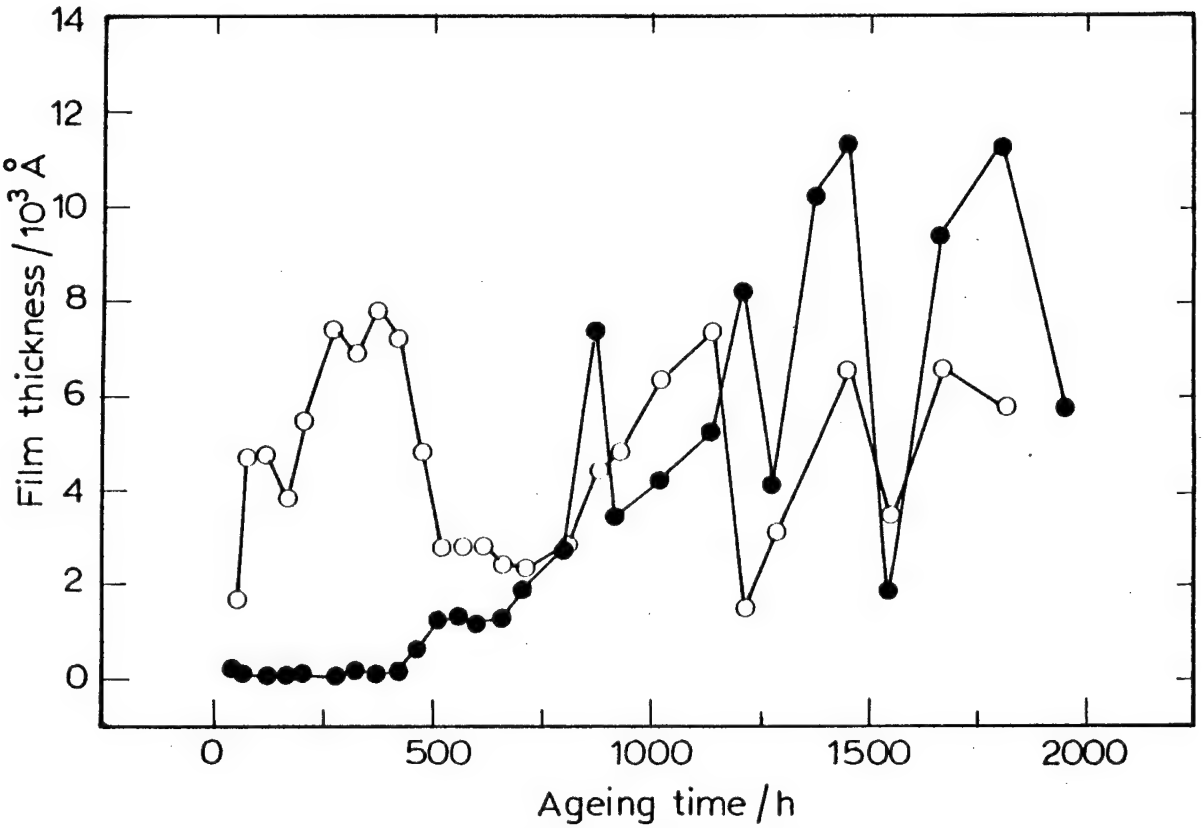

Figure 26. Variation of thickness of passive film formed on lithium in PEO_8LiClO_4 (O) and PEO-PC-$LiClO_4$ (●) solid electrolytes during ambient temperature ageing.

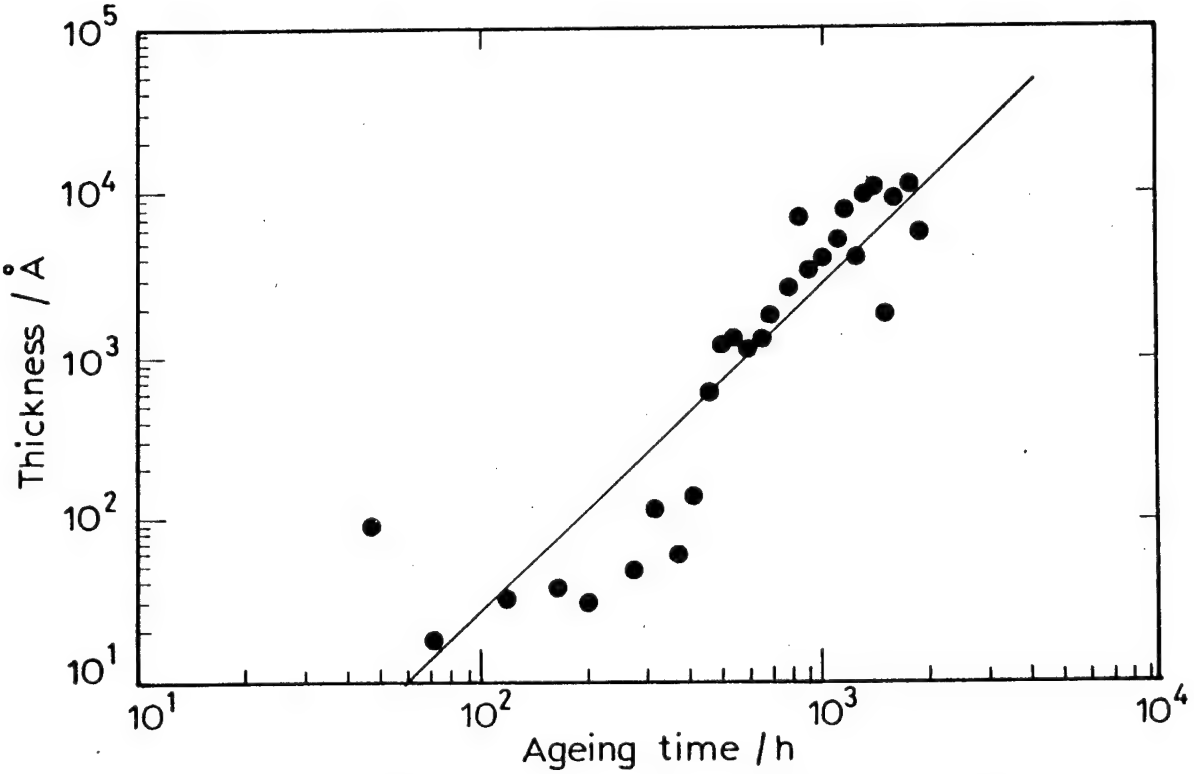

Figure 27. Thickness of passive film on lithium in PEO-PC-$LiClO_4$ electrolyte versus ageing time at ambient temperature in logorithmic scales. Slope of the average linear fit is 1.988 $\pm$ 0.188.

of Li^+ ion concentration in SPE. It is likely that the oxidation of lithium metal takes place at the expense of reductive decomposition of PEO, PC or ClO_4^-. A portion of the oxidized lithium forms passivating layer by combining with reduction products of PEO, PC or ClO_4^-. The remaining portion reaches the SPE and gets coordinated with the oxygen atoms in PEO. As this process leads to ion-pair formation, the conductivity of SPE decreases. The charge-balance within the SPE perhaps is accomplished by the negatively charged decomposed species from PEO, PC or ClO_4^-. The processes that take place at Li/SPE interface are very complex and a direct evidence is lacking for the proposed mechanism.

3.5. Ageing at 80°C followed by ambient temperature ageing of cell 1 and cell 2. EIS studies

Following the storing of cells at ambient temperature for about 2000h, the temperature of the cells was increased and maintained at 80°C over a further period of about 800 h. The cells were subjected to open circuit EIS measurements at several intervals.

The Nyquist plots of both types of cells contained a distorted semi-circle (Fig. 28). The high frequency intercept gave the resistance of the

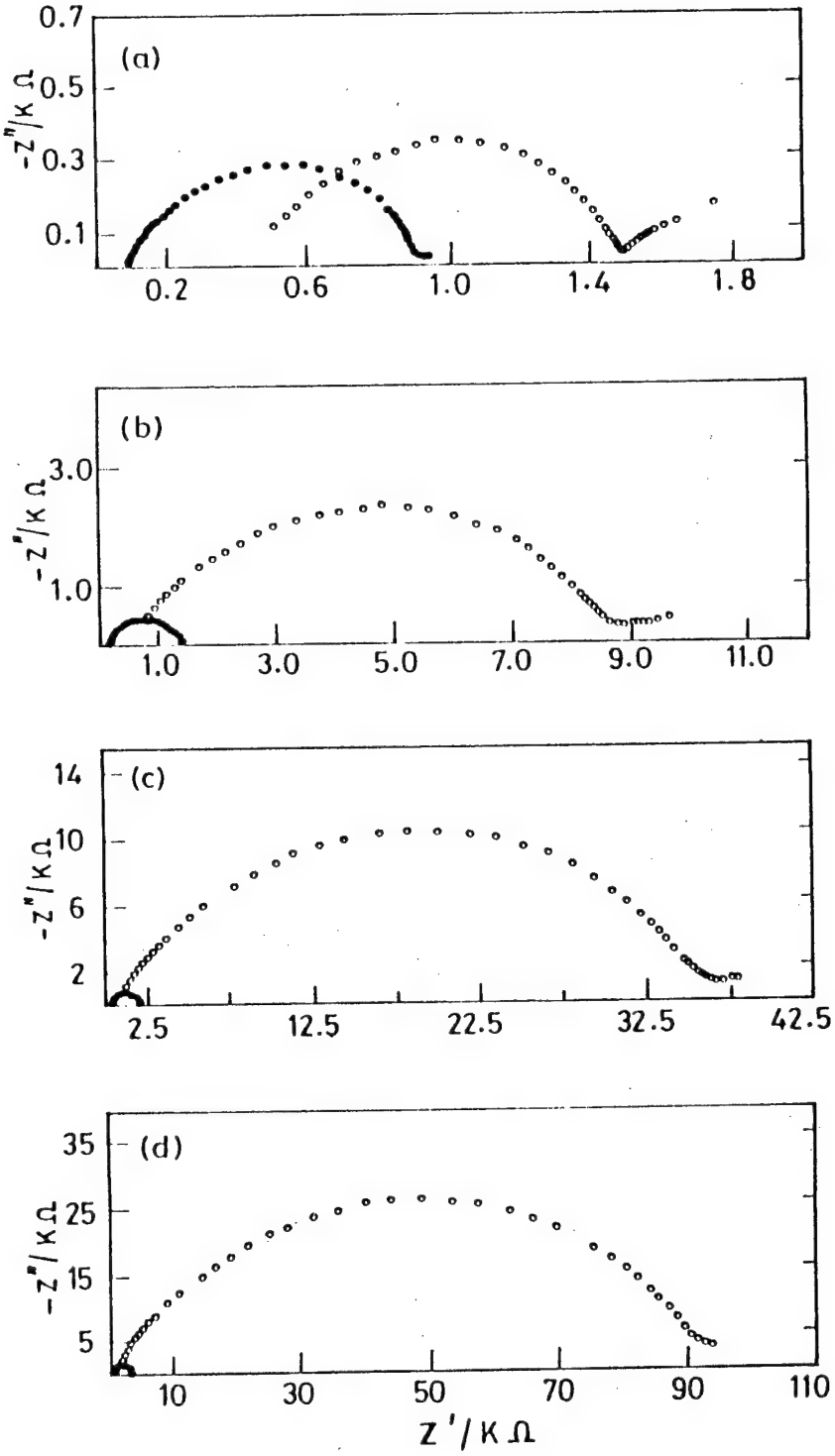

Figure 28. Nyquist plots of Li/PEO_8LiClO_4/Li (●) and Li/PEO-PC-$LiClO_4$/Li (O) at 80°C when the cells were aged for (a) 0 h (b) 15 h (c) 36 h and (d) 60 h.

electrolyte film (R_b), and from the distorted semicircle, the interfacial resistances R_f and R_{ct} were evaluated as described earlier. The variations of R_{cell}, R_f and R_{ct} with the ageing time of cell 1 and cell 2 are shown in Fig. 29 and Fig. 30 respectively. The parameters of both the cells tend to increase during storing at 80°C.

The ageing behaviour of the cells is compared clearly in Fig. 28, in which Nyquist plots for a few typical ageing periods are shown. The Nyquist plot tends to become bigger and bigger for cell 2 in relation to that of cell I as ageing proceeds. The resistances of the cells (R_{cell})are compared and shown in Fig. 31. Both the types of cells have R_{cell} similar in magnitude in the beginning of 80°C storing. On ageing, however, R_{cell} of cell 2 increases to a great extent. The exchange current density (I_o) in both the cells are shown in Fig. 32. I_o is about 8 x 10^{-4} A cm^{-2} in cell 2 and it is 5 x 10^{-5} A cm^{-2} in cell 1 in the beginning of ageing. On ageing, I_o decreases in both the cells. In cell 1, I_o decreases to 10^{-7} A cm^{-2}, whereas in cell 2 it decreases only marginally and remains at 10^{-5} A cm^{-2}.

3.6. Studies on the influence of PC concentration in PEO-PC-$LiClO_4$ solid polymer electrolyte

The influence of PC in PEO-$LiClO_4$ solid polymer electrolyte is studied in more detail by preparing films containing varied concentrations of PC.

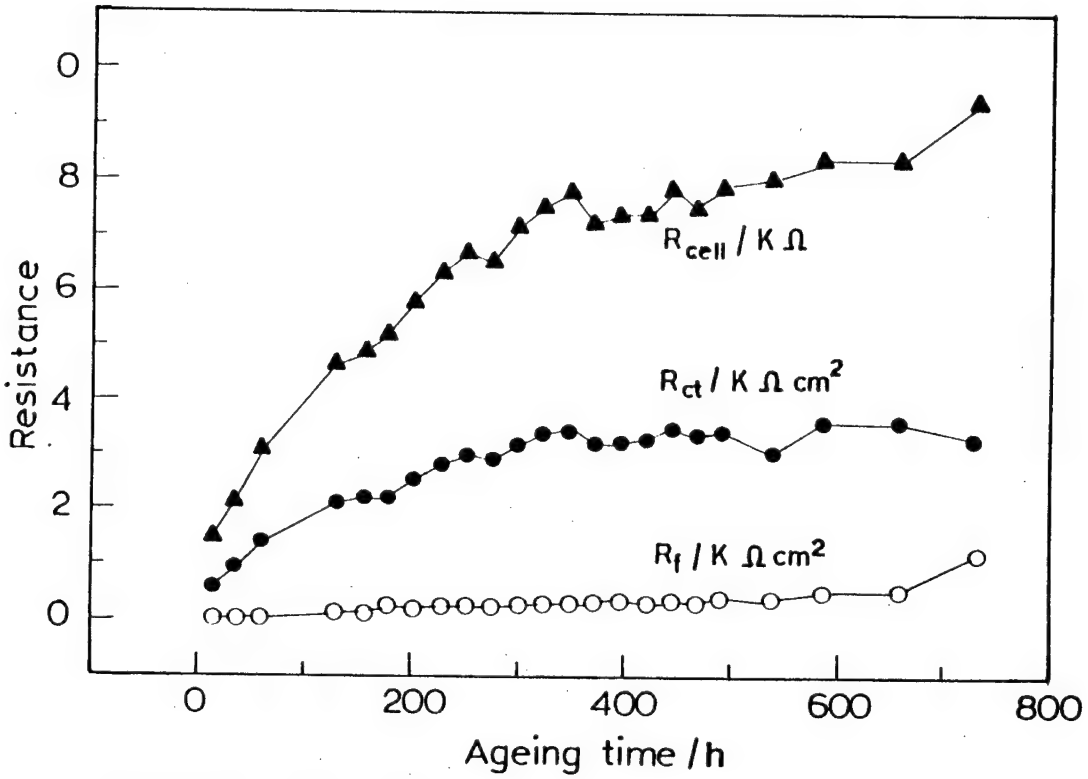

Figure 29. Time evolution of cell resistance (R_{cell}), passive film resistance (R_f) and charge transfer resistance (R_{ct}) evaluated from Li/PEO_8LiClO_4/Li at 80°C.

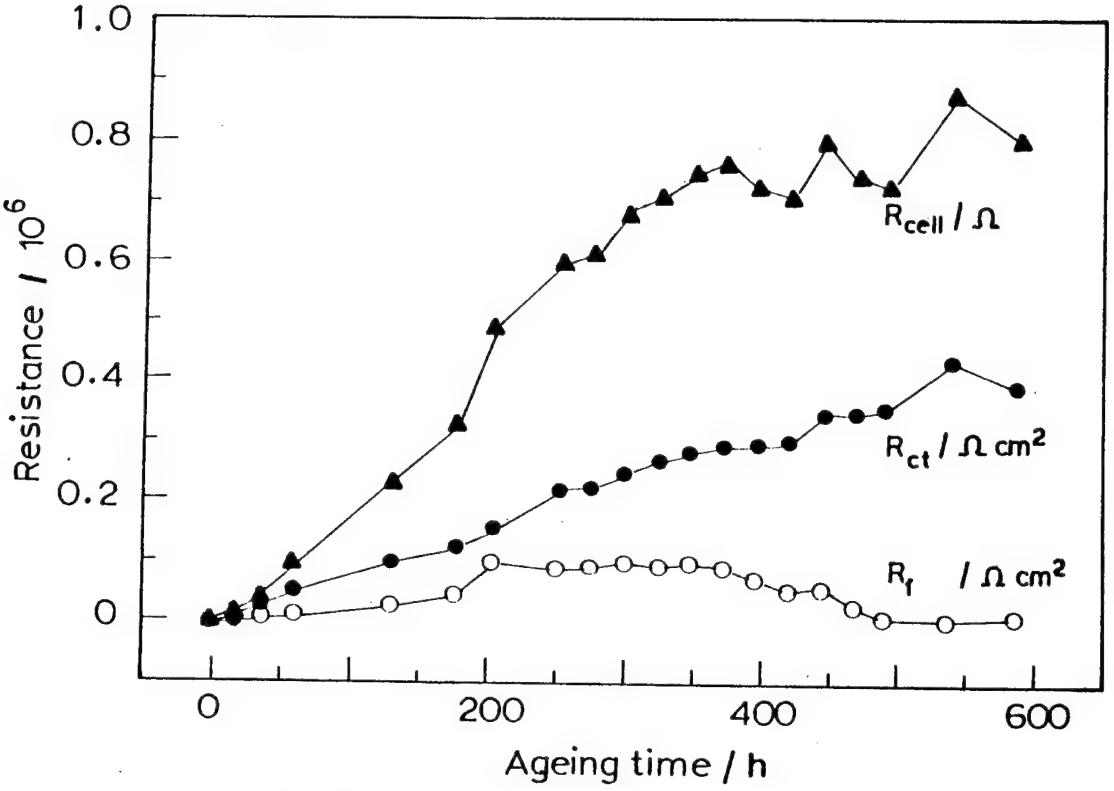

Figure 30. Time evolution of cell resistance (R_{cell}), passive film resistance (R_f) and charge transfer resistance (R_{ct}) evaluated from Li/PEO-PC-$LiClO_4$/Li at 80°C.

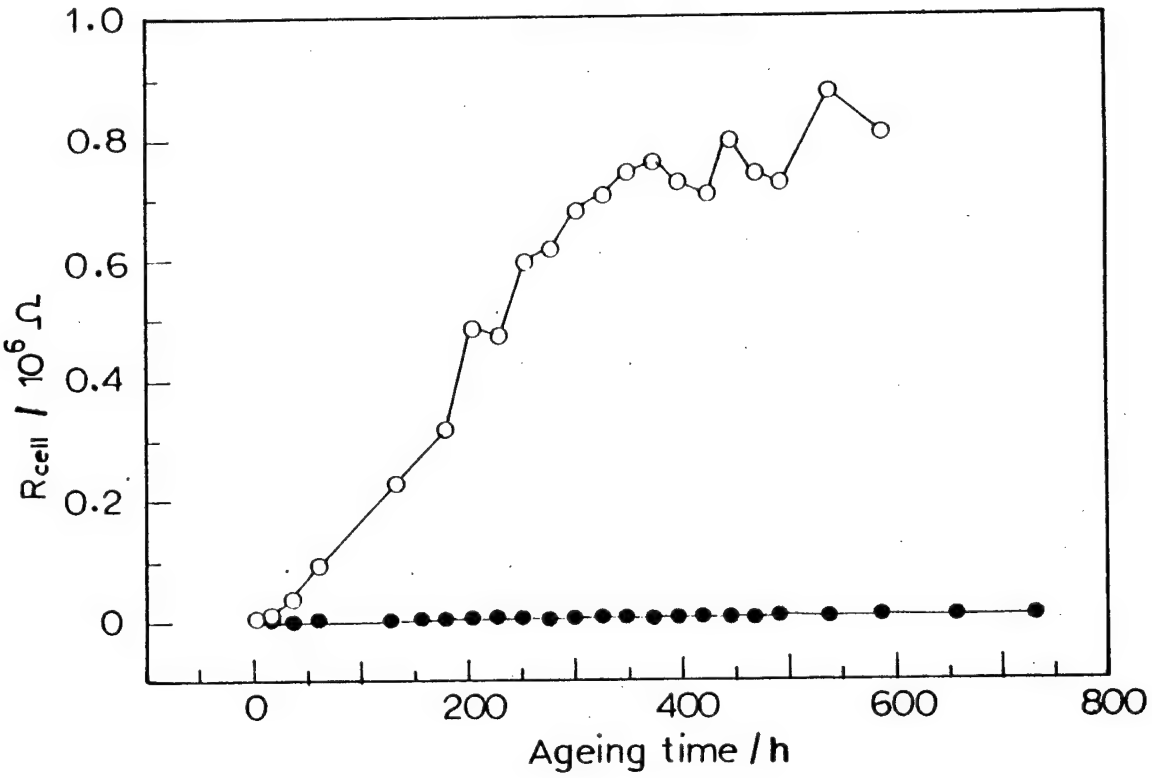

Figure 31. Time evolution of resistance (R_{cell}) of $Li/PEO_8LiClO_4/Li$(●) and Li/PEO-PC-$LiClO_4$/Li(O) at 80°C.

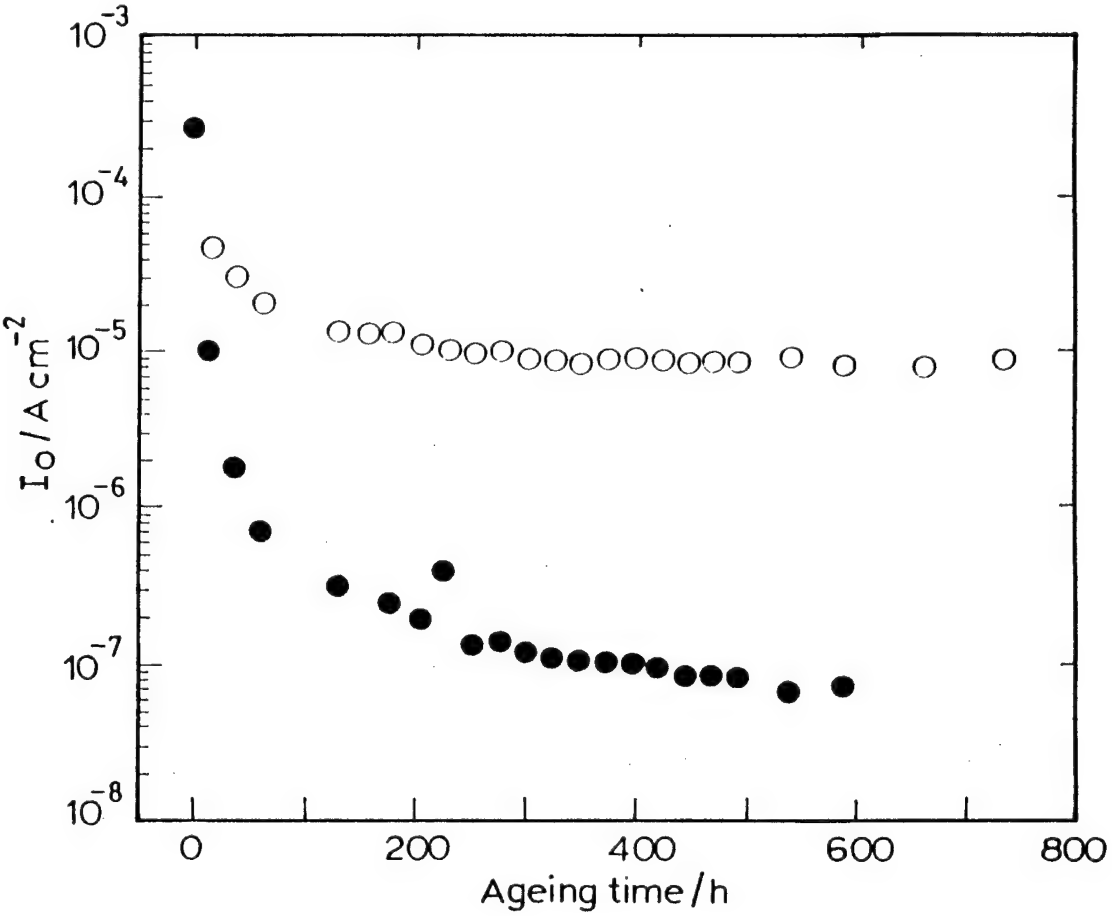

Figure 32. Time evolution of exchange current density (I_o) of $Li^+ + e^- = Li$ reaction in PEO_8LiClO_4(O) and PEO-PC-$LiClO_4$(●) at 80°C.

Symmetrical cells of the type - (i) Li/PEO_8LiClO_4/Li, (ii) Li/PEO-PC-$LiClO_4$ (wt. ratio 1:0.6:0.3)/Li, (iii) Li/PEO-PC-$LiClO_4$ (wt. ratio 1:1.2:0.3)/Li and (iv) Li/PEO-PC-$LiClO_4$ (wt. ratio 1:2.2:0.3)/Li were assembled. These cells are hereafter referred to as cell 3, cell 4, cell 5 and cell 6 respectively. The cells were aged at 80°C and EIS measurements were carried out at several intervals of ageing. At some intervals of ageing at 80°C, the EIS measurements were also carried out at several decreased temperatures in order to evaluate Arrhenius behaviour of internal cell parameters such as R_f, R_{ct} and I_o.

The Arrhenius plots of R_f, R_{ct} and I_o of cell 3 are shown in Fig. 33 and Fig. 34 at two different ageing intervals. The parameters R_f and R_{ct} decrease and I_o increases with an increase of temperature. Employing Arrhenius equation, energy of activation (E_a) of the processes corresponding the three parameters are calculated. The R_f, R_{ct} and I_o of cell 4, cell 5 and cell 6 were also found to follow Arrhenius equation, the corresponding plots are shown in Figs. 35-40. The E_a values obtained from Figs. 33-40 are given in the Table I.

The value of E_a of R_f at 50 h of ageing for cell 3 is the highest in relation to the cell 4, cell 5 and cell 6. Additionally, E_a increases with an increase

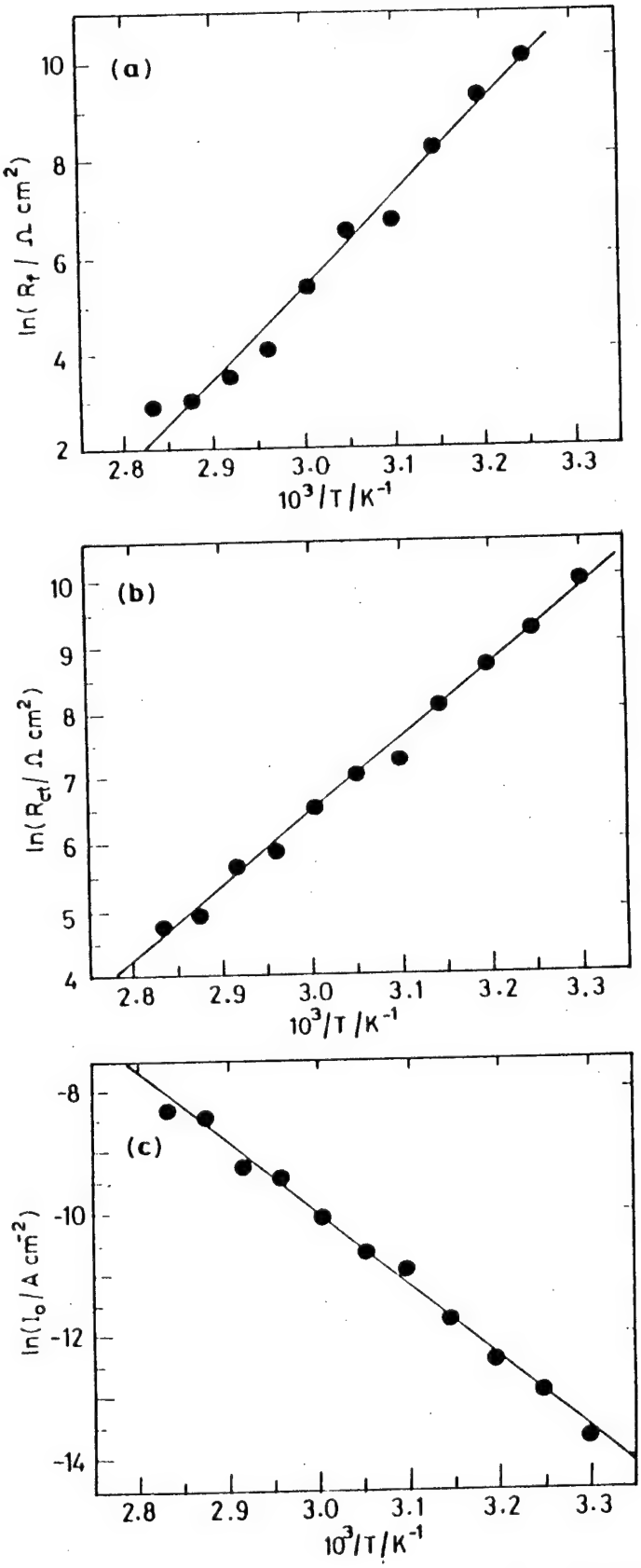

Figure 33. Arrhenius plots of (a) passive film resistance (R_f), (b) charge transfer resistance (R_{ct}) and (c) exchange current density (I_o), which were evaluated from Li/PEO_8LiClO_4/Li cell (cell3). The cell was aged at 80°C for 50 h.

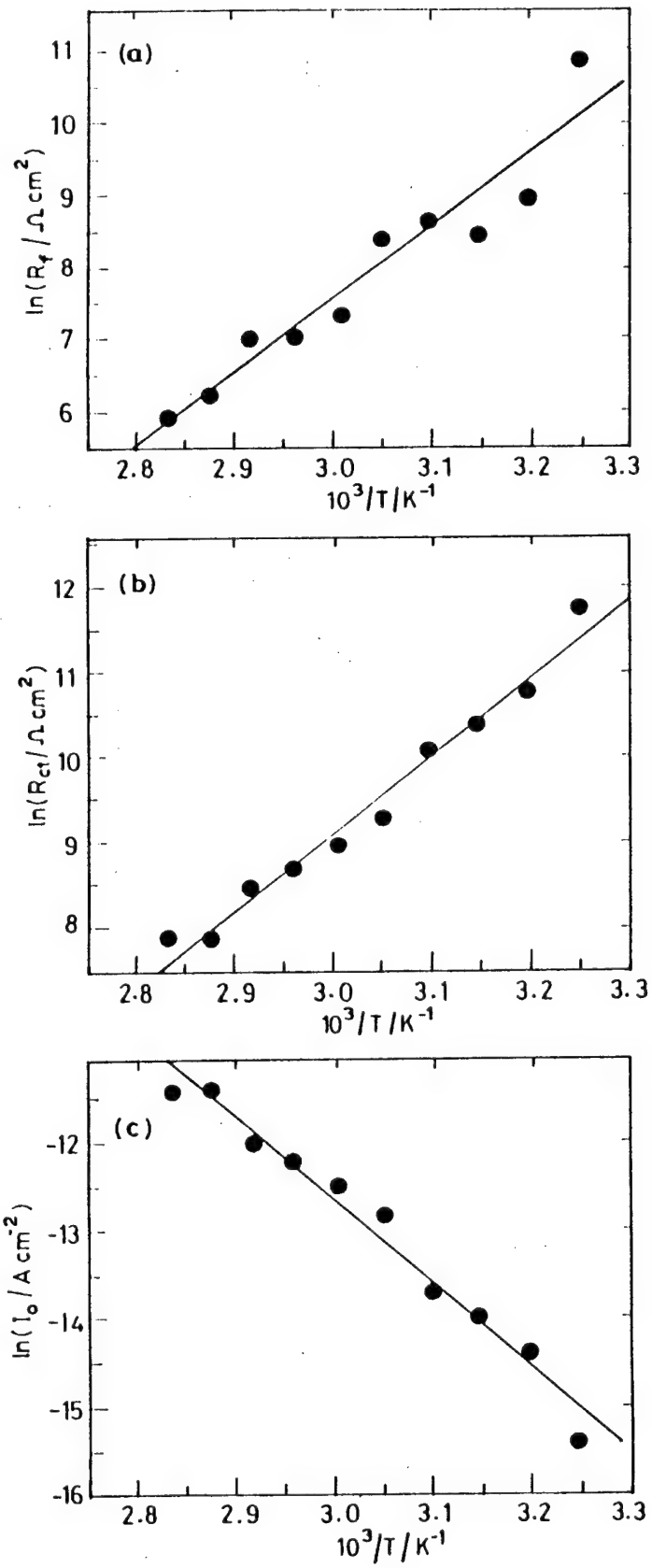

Figure 34. Same as Figure 33, except that the cell was aged at 80°C for 530 h.

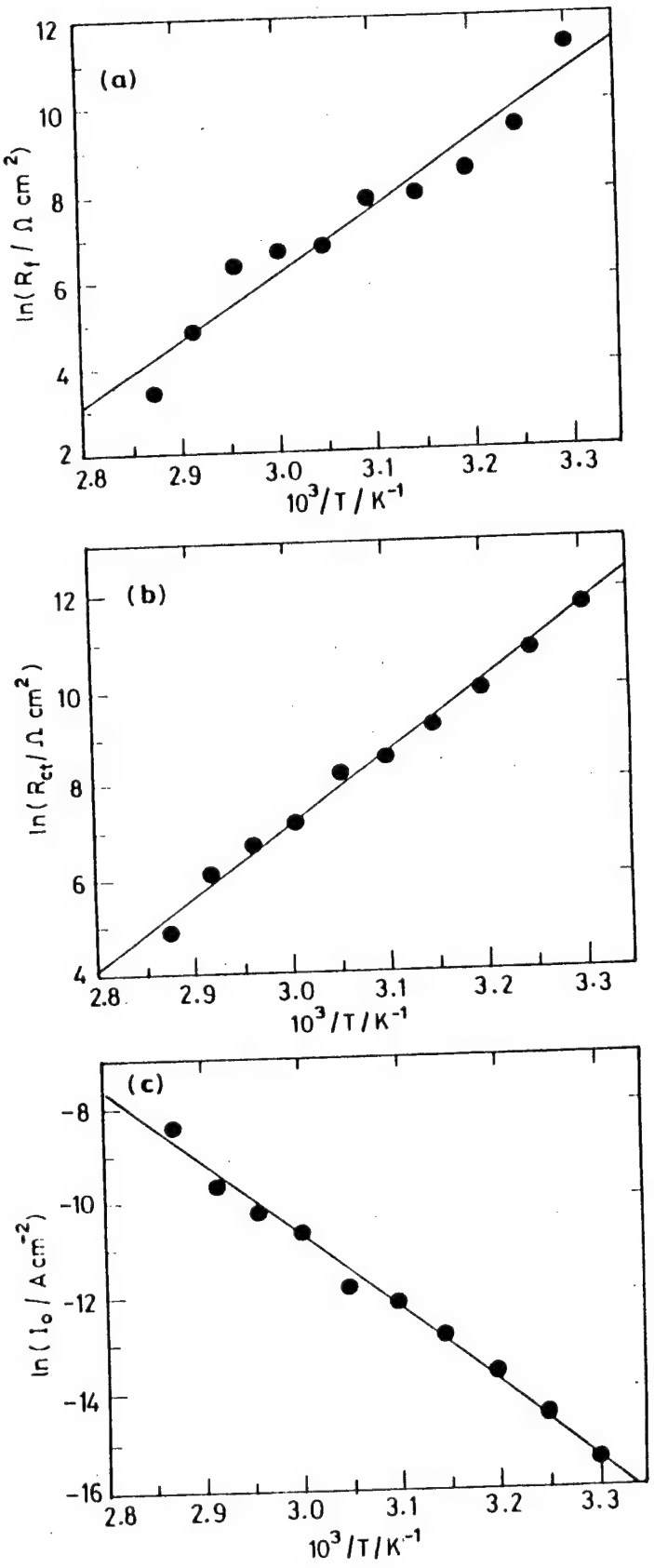

Figure 35. Arrhenius plots of (a) passive film resistance (R_f), (b) charge transfer resistance (R_{ct}) and (c) exchange current density (I_o), which were evaluated from cell4. The cell was aged at 80°C for 50 h.

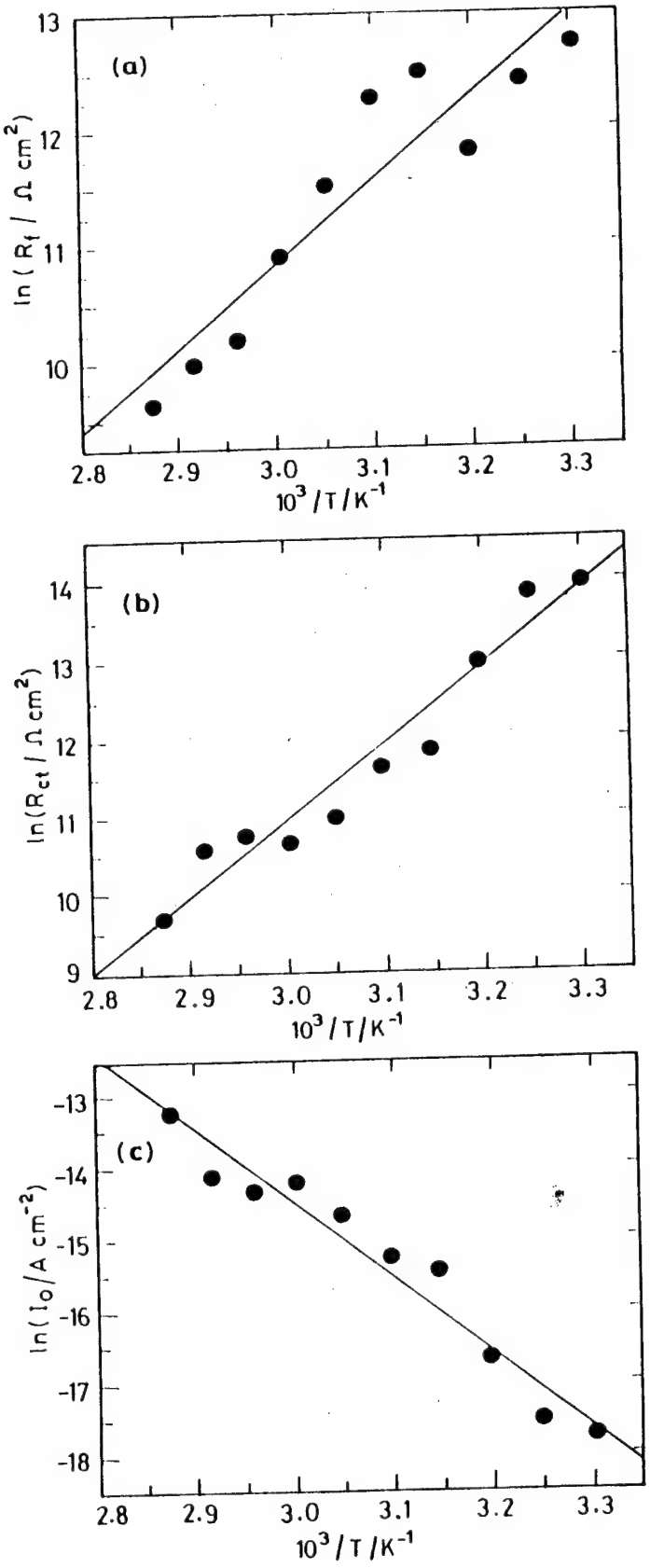

Figure 36. Same as Figure 35, except that the cell was aged at 80°C for 530 h.

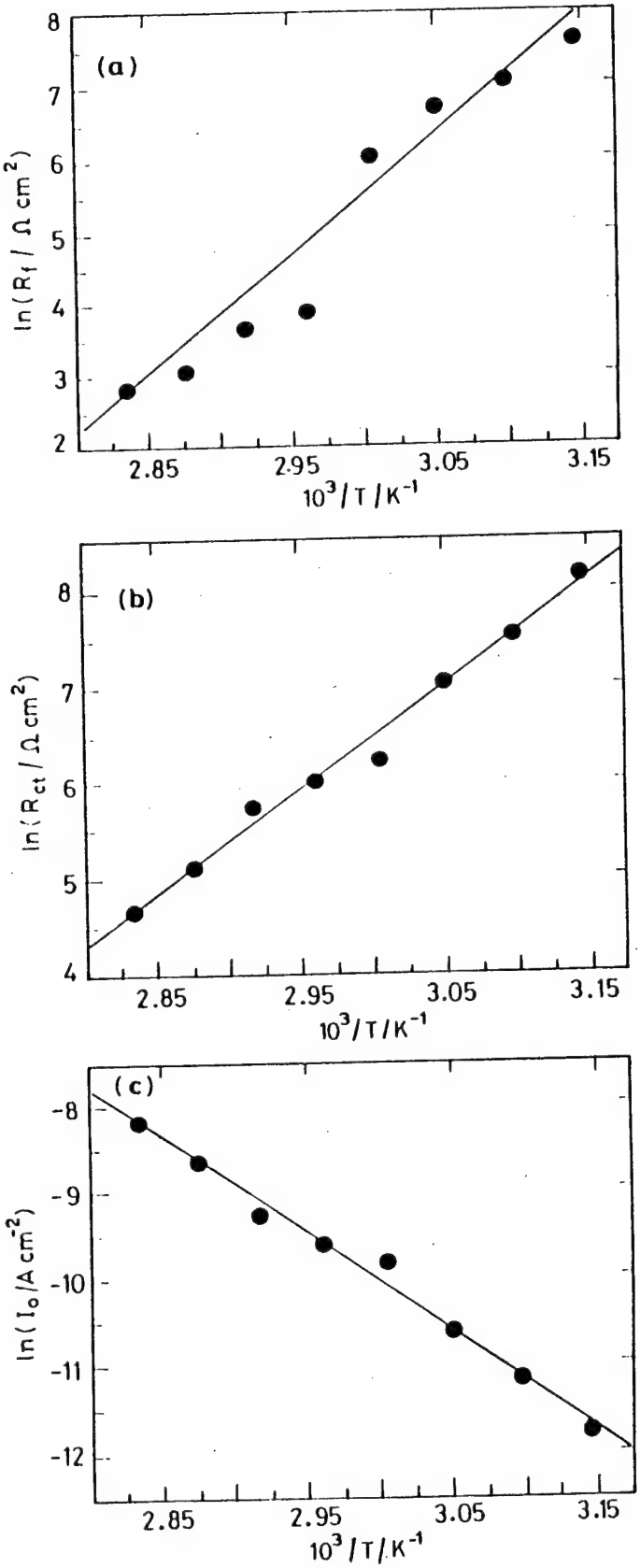

Figure 37. Arrhenius plots of (a) passive film resistance (R_f), (b) charge transfer resistance (R_{ct}) and (c) exchange current density (I_o), which were evaluated from cell5. The cell was aged at 80°C for 50 h.

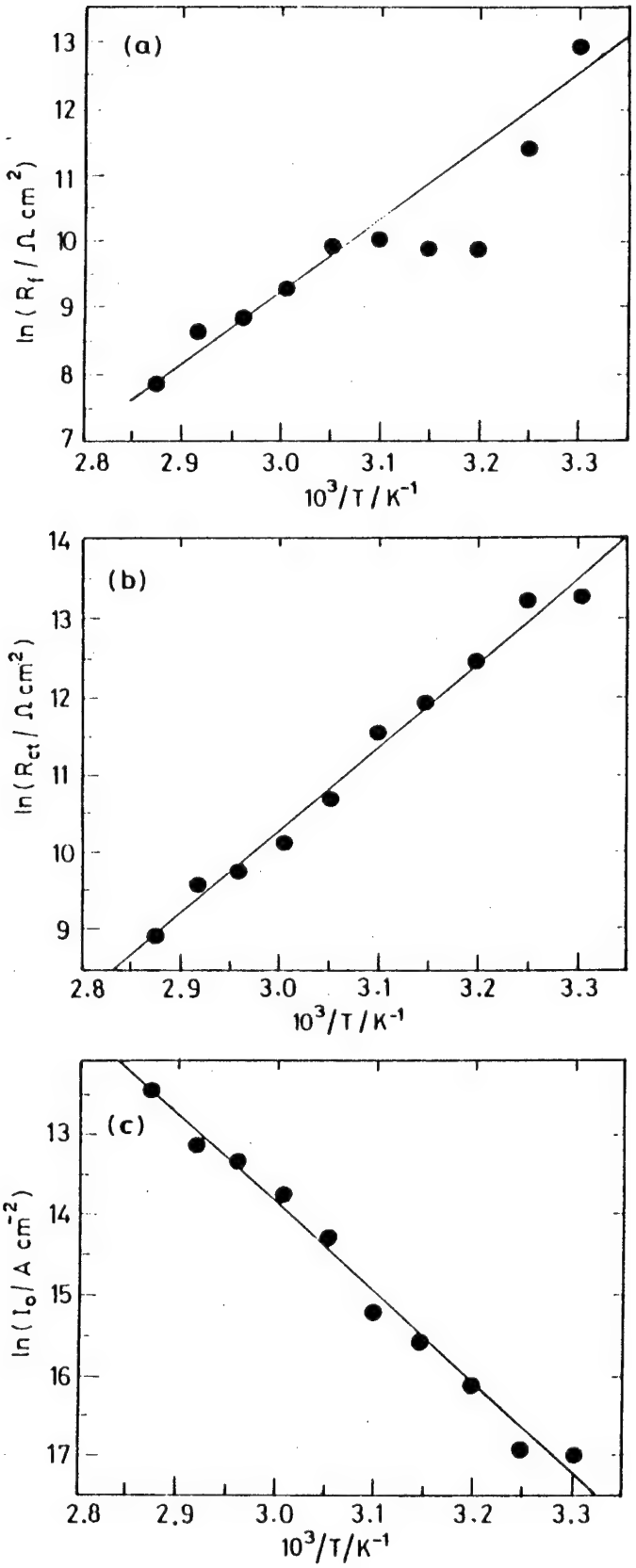

Figure 38. Same as Figure 37, except that the cell was aged at 80°C for 530 h.

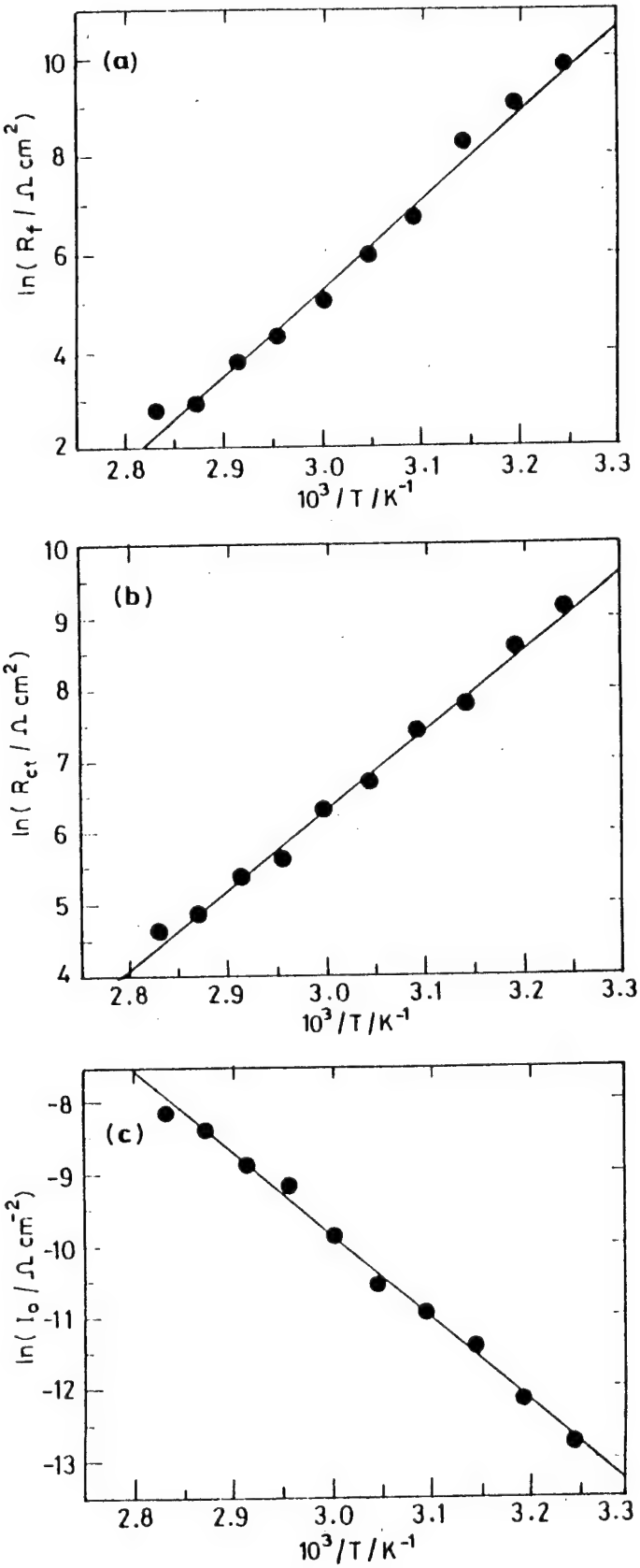

Figure 39. Arrhenius plots of (a) passive film resistance (R_f), (b) charge transfer resistance (R_{ct}) and (c) exchange current density (I_o) which were evaluated from cell6. The cell was aged at 80°C for 50 h.

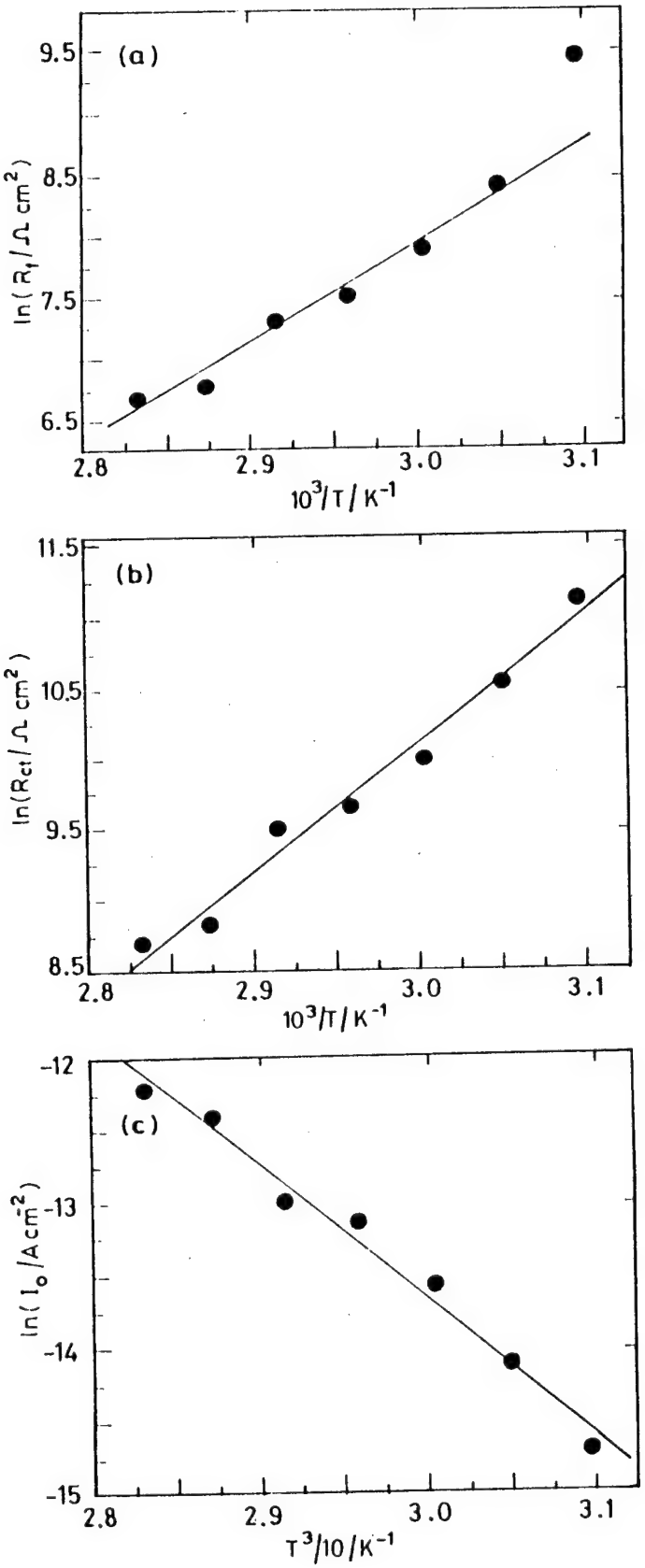

Figure 40. Same as Figure 39, except that the cell was aged at 80°C for 530 h.

Table I

The values of energy of activation (E_a) evaluated from Arrhenius plots (Figs. 33-40).

Para-meters	Ageing	E_a/eV			
		cell 3	cell 4	cell 5	cell 6
R_f	50 h	-1.612±0.074	-1.302±0.114	-1.484±0.149	-1.529±0.058
	530 h	-0.887±0.092	-0.636±0.089	-0.792±0.114	-0.840±0.95
R_{ct}	50 h	-0.975±0.024	-1.289±0.044	-0.935±0.040	-0.947±0.028
	530 h	-0.7935±0.046	-0.854±0.075	-0.935±0.043	-0.785±0.052
I_o	50 h	0.999±0.013	1.318±0.043	0.960±0.043	0.963±0.044
	530 h	0.82±0.047	0.8905±0.0745	0.965±0.043	0.8096±0.052

of the PC concentration in PEO_8LiClO_4. These observations suggest that the composition of the passive film depends on the amount of PC present in PEO_8LiClO_4. On ageing, i.e., at 540 h, E_a of R_f in all the cases decreases. An easy and less energetic path or mechanism of conduction in the aged passive films are inferred. In an analogous manner, the energy of activation for the electrochemical reaction across the interface also decreases when the cells are aged.

3.7. Studies on the influence of concentration of lithium salt in SPE on the exchange current of $Li^+ + e^- = Li$ reaction

It is discussed in Section 3.2 about the effect of concentration on the exchange current of an electrochemical reaction. It is further shown that I_o of $Li^+ + e^- = Li$ reaction in liquid electrolytes follows the expected trend in different concentrations of the lithium salt.

In the present investigations, films of the following compositions were prepared. PEO, $PEO_{32}LiClO_4$, $PEO_{16}LiClO_4$, PEO_8LiClO_4 and PEO_4LiClO_4. The concentration of Li^+ in these electrolytes are respectively 0, 0.55, 1.09, 2.08 and 3.82 mol l^{-1}, which were calculated based on density of PEO and $LiClO_4$. Symmetrical cells were fabricated and impedance measurements

were carried out at 80°C. The I_o of $Li^+ + e^- = Li$ reaction is shown as a function of Li^+ in SPE (Fig. 41). The ln I_o is not linear with lnC, in contrast to eqn.23. I_o is found to be maximum in PEO_8LiClO_4 electrolyte and it is lower in the other electrolyte films. At concentrations lower than 2.08 mol/l (i.e., in PEO_8LiClO_4), the lesser value of I_o is attributed to low concentrations of Li^+ in SPE. The decreased value of I_o at higher concentrations is probably due to ion-pair formation, thus the effective concentration of Li^+ is less.

3.8. Studies on hybrid solid polymer electrolytes consisting of PEO and PAN

The aim of the present investigations was to prepare dry and dimensionally stable HSPE films and to characterize them for ionic conductivity as well as the electrochemical reaction occurring at Li/HSPE interface. While the SS/HSPE/SS cells were used for conductivity measurements, the (SS)Li/HSPE/Li(SS) were employed for studies related to the electrochemical reaction.

It was intended to arrive at an appropriate composition of HSPE on the basis of high specific conductivity achievable while the HSPE film was dry with good dimensional stability. The HSPE consists of several components, viz., PEO, PAN, PC, EC and $LiClO_4$, and therefore experiments required for arriving at the appropriate composition, taking account of all components and their

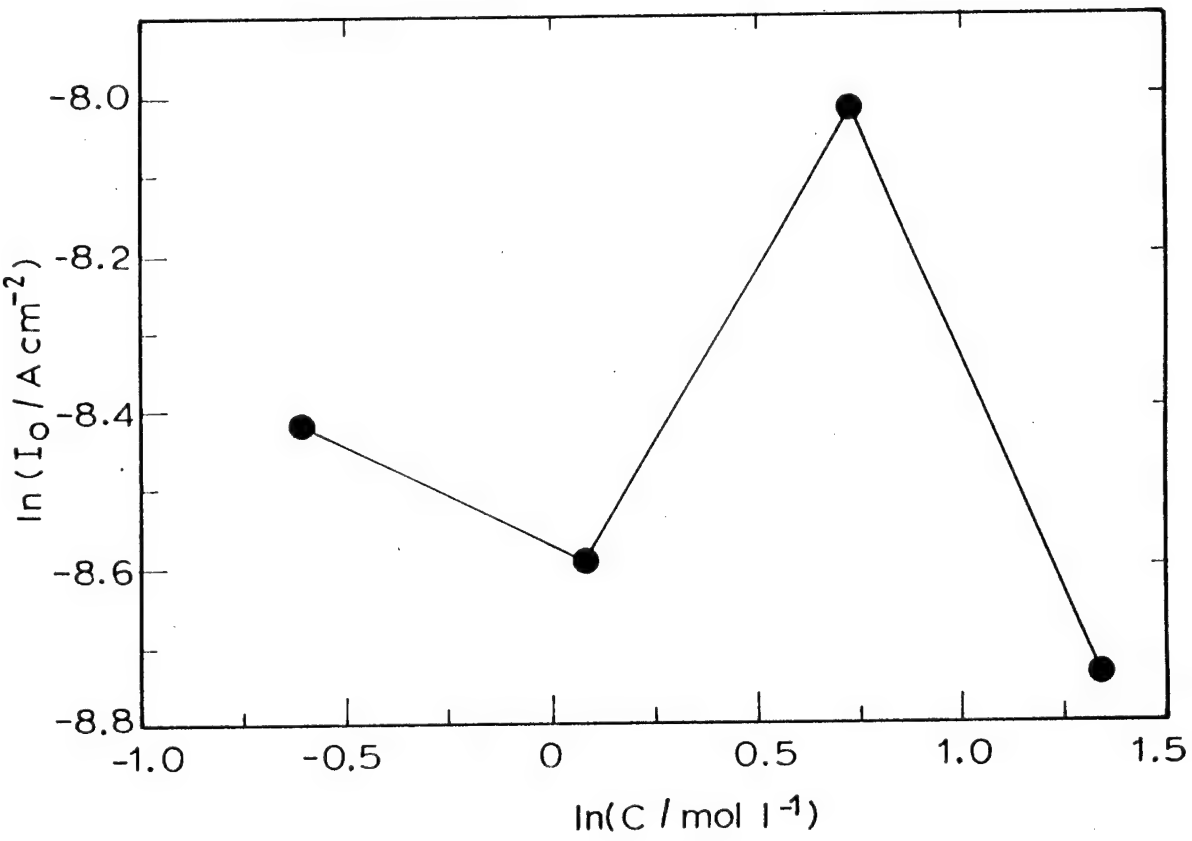

Figure 41. Exchange current density (I_o) as a function of concentration (C) of lithium perchlorate in PEO solid polymer electrolyte at 80°C.

contributions, are rather large in number. As the enhancement in conductivity is considered due to the presence of PC and EC, several HSPE films were prepared only varying the concentration of PC and EC while maintaining concentrations of other components nearly invariant. The conductivity (σ) of the HSPE films as a function of mole ratio of (PC + EC)/$LiClO_4$ is shown in Fig. 42 at different temperatures. It is evident that the HSPE film having 3.67 mole ratio of (PC + EC)/$LiClO_4$ exhibits the highest conductivity at all temperatures. The composition of this film with σ = 0.37 mS cm^{-1} at 30°C is shown in Table II, together with the composition of PEO + PC and PAN + PC + EC electrolyte films. The conductivity (σ = 0.37 mS cm^{-1}) of the HSPE film is slightly less than σ (=0.84 mS cm^{-1}) of PEO + PC and σ (=1.34 mS cm^{-1}) of PAN + PC + EC films. The advantage, however, is that the HSPE film is dry with good mechanical stability.

It is clear from the composition of the HSPE as well as from IR spectrum that ionic conduction should, in principle, occur parallely on two different paths viz., segmental motion of PEO chains and ionic mobility in liquid medium (PC and EC). The relative contribution of these two paths, however, is not reflected in the impedance diagrams. It is probably due to the fact that there is a wide difference in σ of the two paths. The value of σ is about 10^{-8} S cm^{-1} in PEO-$LiClO_4$ medium, whereas it is about 10^{-3} S cm^{-1} or higher in PC-EC-$LiClO_4$ medium at ambient temperature.

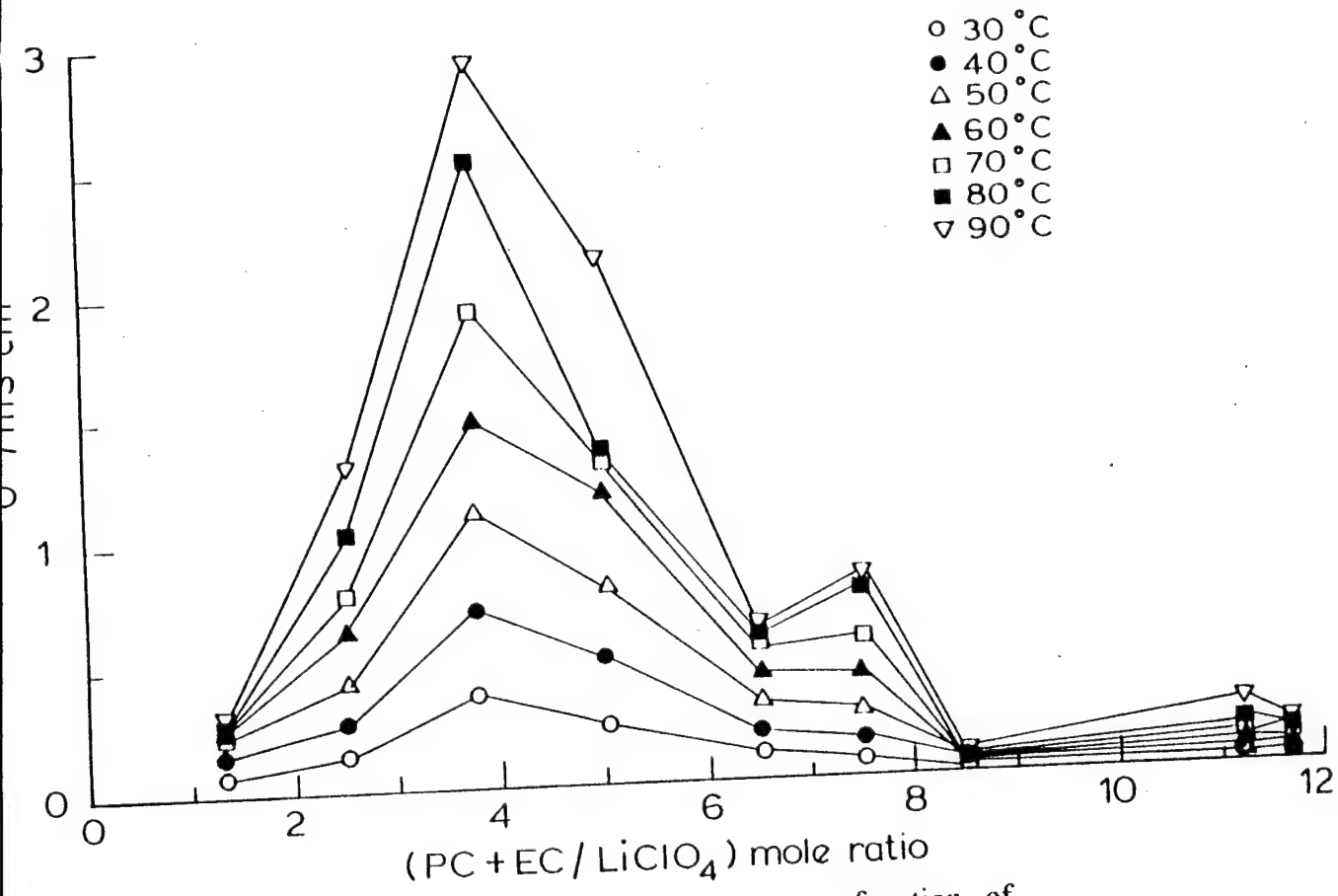

Figure 42. Specific conductivity (σ) as a function of ($PC+EC/LiClO_4$) mole ratio at different temperatures.

TABLE II

The composition of polymer electrolyte films with specific conductivity (σ) and exchange current density (I_o) of lithium electrode reaction at 30°C.

Film	Composition			σ	I_o
	Component	in mM	in gram	mS cm^{-1}	$\mu A\ cm^{-2}$
(I) HSPE					
	PEO	22.7	1.000	0.37	1.3
	PAN	17.4	0.750		
	PC	7.3	0.750		
	EC	8.5	0.750		
	$LiClO_4$	4.3	0.450		
(II) PEO+PC					
	PEO	22.7	1.000	0.84	11.0
	PC	13.3	1.366		
	$LiClO_4$	1.2	0.123		
(III) PAN+PC+EC					
	PAN	23.2	1.000	1.34	3.7
	PC	24.5	2.500		
	EC	28.4	2.500		
	$LiClO_4$	3.0	0.320		

NOTE : mM of PEO and PAN are calculated based on the molecular weight of a repeat unit of the polymer.

The temperature dependence of σ of the three films given in Table II is shown in Fig. 43. The results are found to follow the Arrhenius relation. The energies of activation of conduction for films numbered I, II and III in Table II are 33.8, 25.2 and 25.9 kJ mol^{-1} respectively. Similar values of activation energy are reported for PAN-based electrolytes.

The values of exchange current density (I_o) of reaction (3) at 30°C in the three electrolytes are given in Table II. The value of I_o is slightly lower in HSPE than in PEO+PC and PAN+PC+EC electrolyte films. Exchange current values about three orders of magnitude higher than the present values were reported for reaction (3) in similar highly conducting polymer or gelled electrolyte films [11]. These studies, however, were made with freshly deposited lithium on a nickel substrate. The lower values of I_o obtained in the present studies can be attributed to a native surface passive film present on Li used for making the cells. The cyclic voltammograms recorded at scan rates ranging from 10-200 mV s^{-1} did not contain current peaks in both cathodic and anodic potential sweeps. Instead, steady-state type of voltammograms with limiting currents were obtained. This suggests that the electron-transfer rate is slower than the rate of diffusion of Li^+ ions at the Li/SPE interface. These observations prevailed in the three types of electrolyte films. The reason for not obtaining current peaks is probably due to

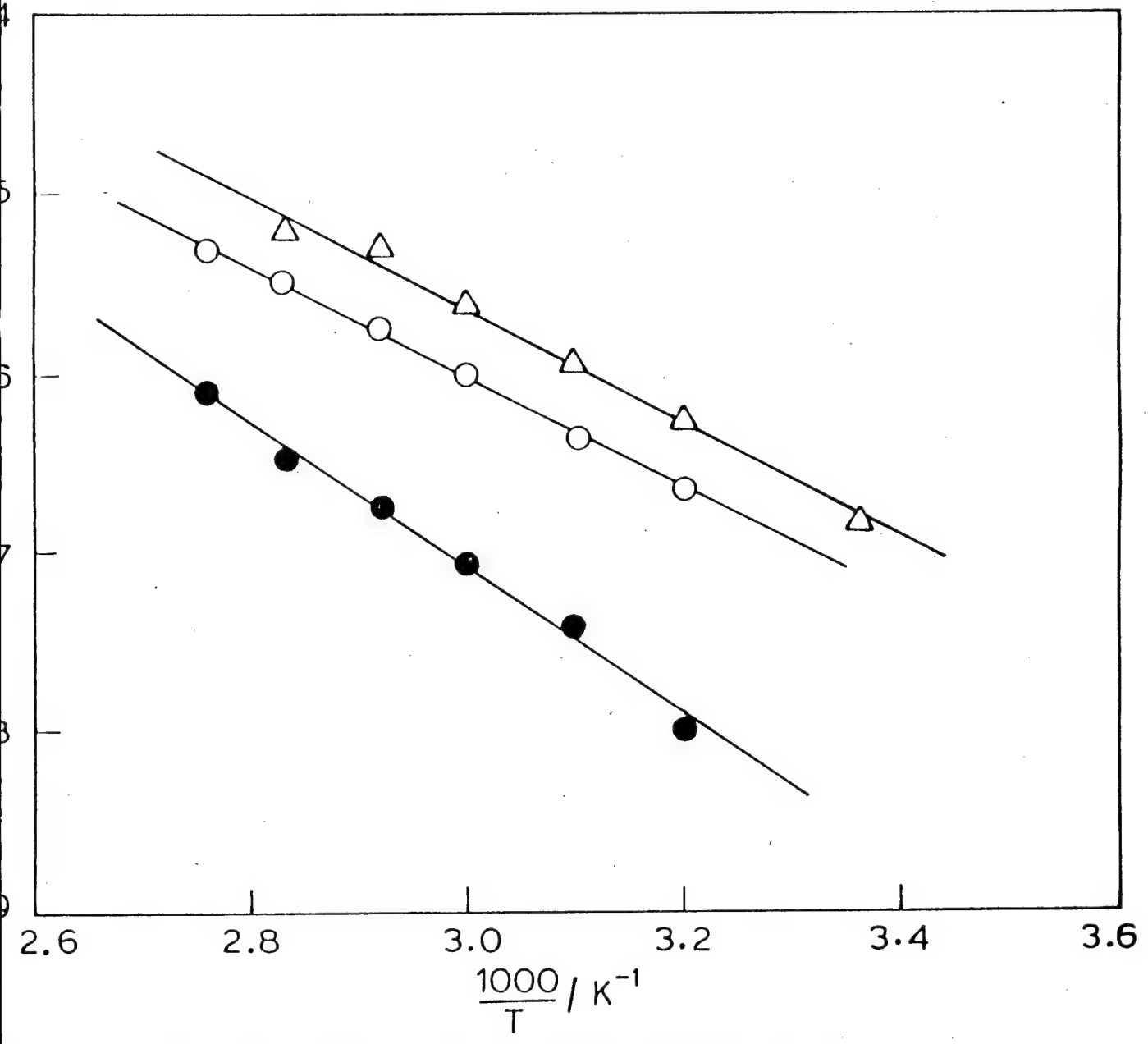

Figure 43. Arrhenius plots of specific conductivity (σ) of HSPE(●), PEO+PC(O) and PAN+PC+EC(△) electrolyte films.

highly resistive passive film which was already formed on Li before recording voltammograms. The cells were sufficiently aged and subjected to high temperature measurements prior to recording voltammograms. These factors are perhaps responsible for the presence of resistance and thicker passive layer on Li.

The complex plane impedance plots at different intervals of ambient temperature ageing of a (SS)Li/HSPE/Li(SS) cell are shown in Fig. 44. It is seen that both the high and low frequency intercepts on real axis keep shifting towards higher values. The specific conductivity (σ) and the interfacial resistance (R_i) are shown as a function of ageing time in Figs. 45 and 46 respectively. It is seen that while σ decreases, R_i increases. When Li metal is in contact with the solid polymer electrolyte film, it tends to undergo oxidation (or corrosion) and the reaction products accumulate resulting in the formation of passive film on Li. As the ageing time progresses, the passive film grows in thickness. Since the reaction (2) has to proceed through the passive film, it experiences a higher resistance (R_i) with increasing ageing time. As a result, exchange current density of the reaction decreases.

The decrease in σ (Fig. 45) is also attributed to the corrosion of Li metal. The three types of electrolyte films contain liquid components (viz., PC and EC) in addition to the solid PEO solvent. It is known that Li is

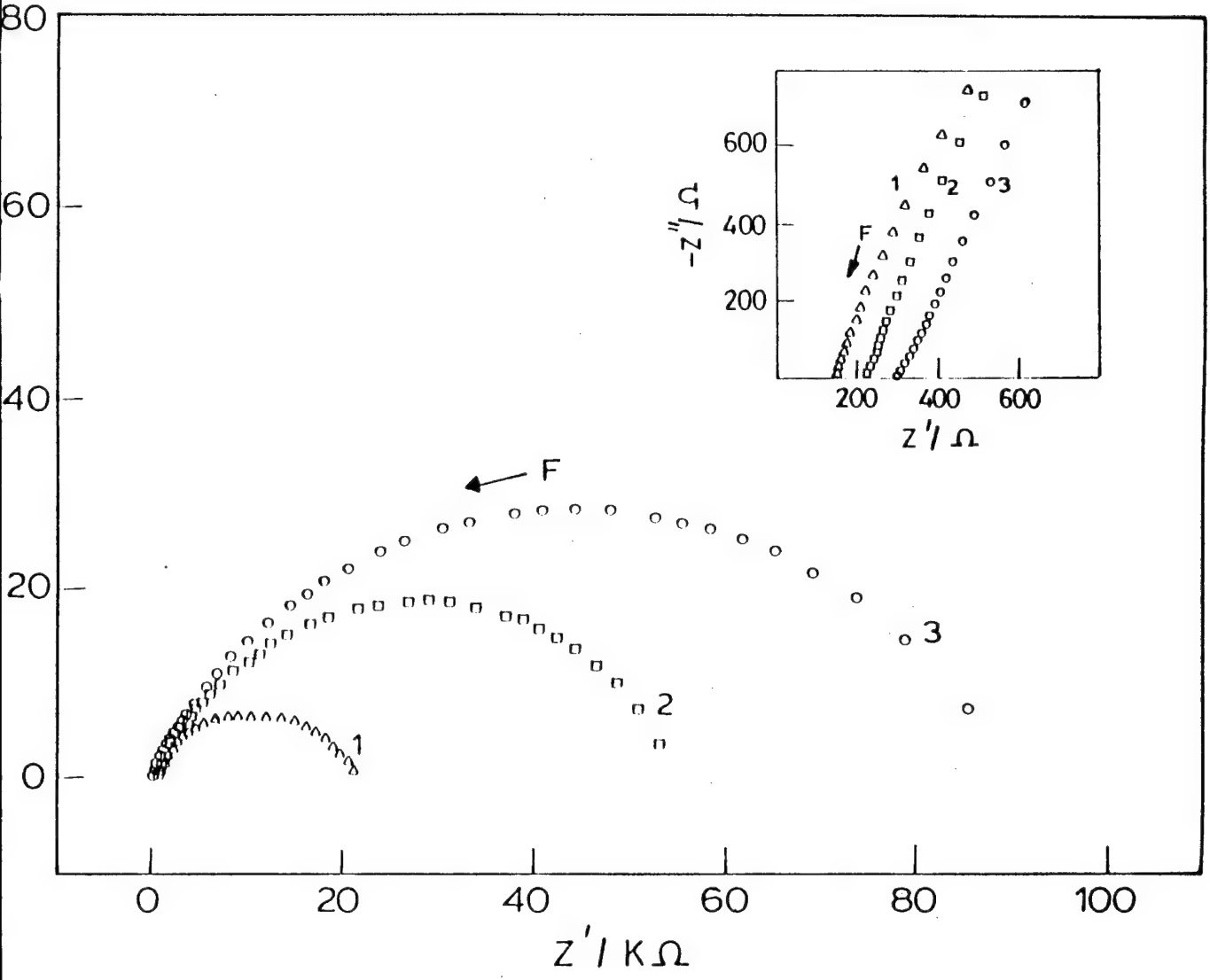

Figure 44. Nyquist plots of (SS)Li/HSPE/Li(SS) cell measured at 48h (1), 144h (2) and 312h (3) after the cell was assembled and aged at ambient temperature. The high frequency intercept is expanded and shown as inset.

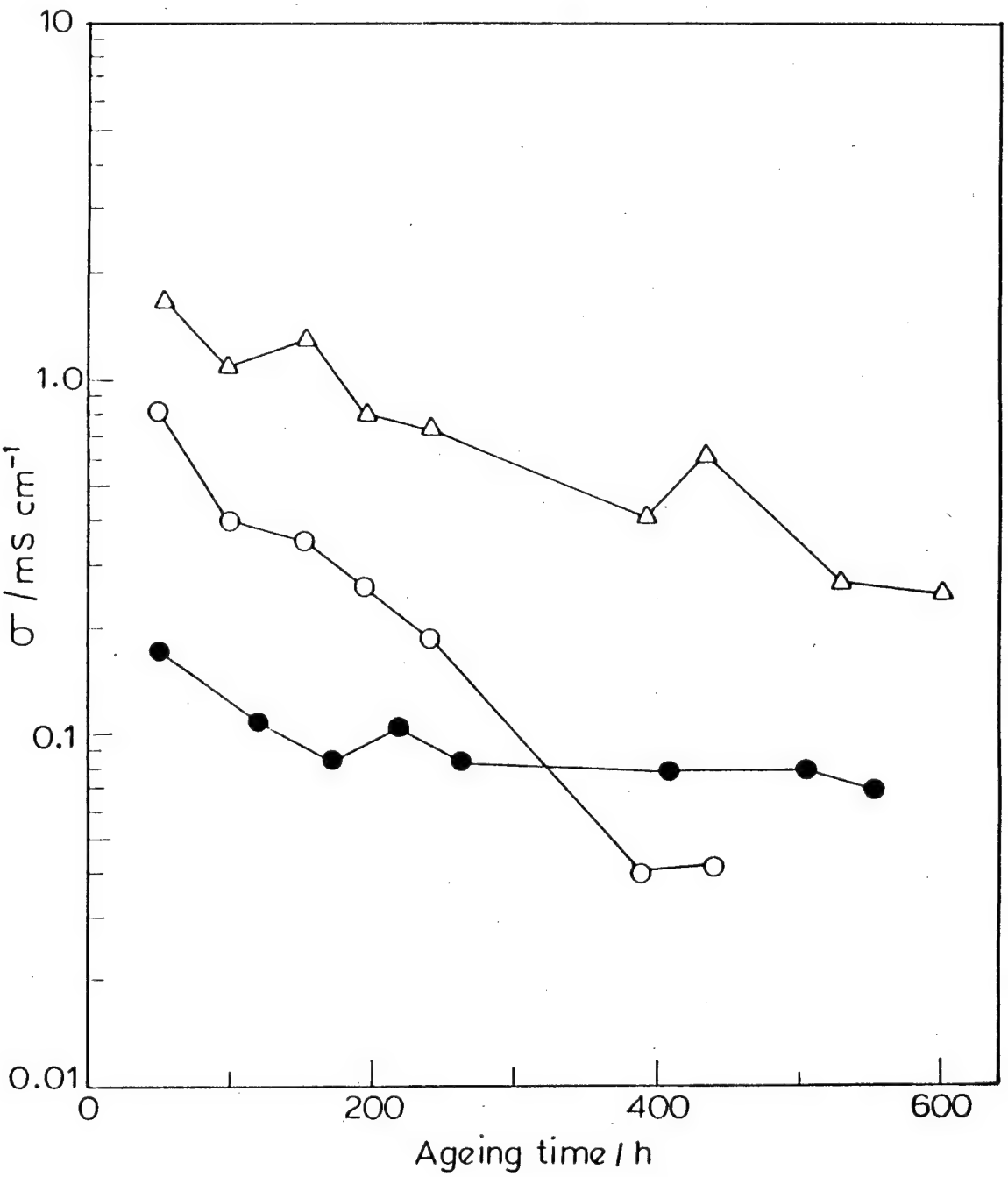

Figure 45. Specific conductivity (σ) of HSPE (●), PEO+PC(O) and PAN + PC + EC (Λ) electrolyte films as a function of ageing time at ambient temperature.

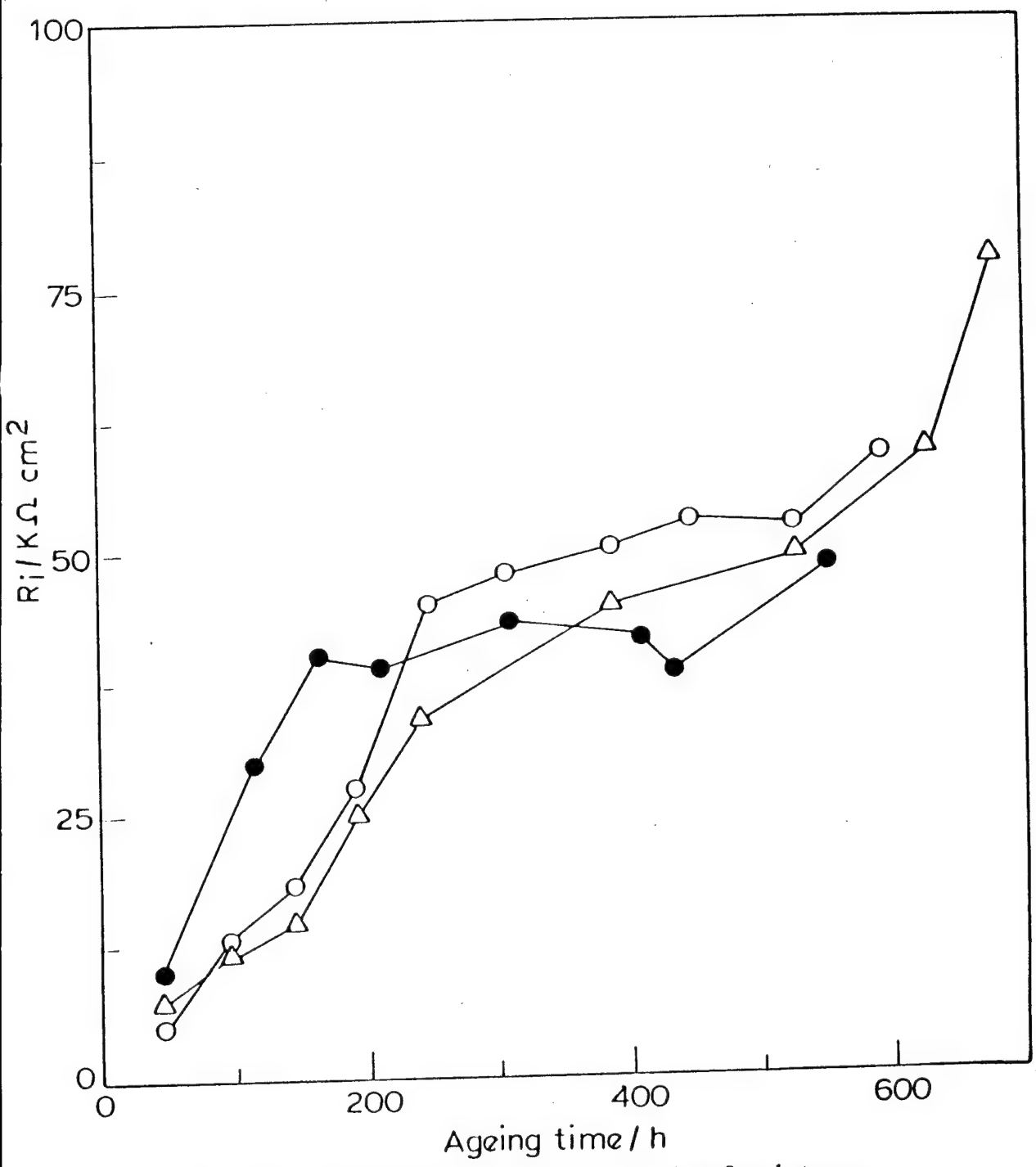

Figure 46. Interfacial resistance (R_i) at the interface between Li and HSPE (●), PEO + PC (O) and PAN + PC + EC (Δ) electrolyte films as a function of ageing time at ambient temperature.

thermodynamically unstable when in contact with PC or EC electrolytes. The liquid solvent molecules undergo reductive decomposition which in turn facilitates the oxidation of Li metal. The decrease in σ on ageing may be due to loss of PC and EC molecules in the electrolyte film. This process leads to changes in composition of the electrolyte film with respect to liquid phase and overall Li^+ ion concentration in the composite medium. The concentration of Li^+ ions can also be considered to change due to partial and slow dissolution of outer layers of passive film into the electrolyte medium. Cells containing the three types of electrolyte films show similar behaviour on ageing. During the course of ageing, the cells were occasionally heated to several temperatures up to 100°C for the purpose of impedance and cyclic voltammetric measurements. All cells, however, were not uniformly subjected to heating and cycling. Since heating and cycling of the cells influence the passive film on Li, and passive film in turn influences σ and R_i, the results shown in Figs. 45 and 46 are only qualitative in nature.

From the FT-IR spectrum of a thin film of HSPE, peaks are assigned by comparing this spectrum with the spectra of individual components of the HSPE, which are reported in the literature. The transmittance band at wave number 555 cm^{-1} is assigned to C=N of PAN. The sharp peak at 632 cm^{-1} is due to complex bond formed between O of PEO chain and Li^+ ion. The peak at wave number 958 cm^{-1} is likely to be due to Li^+-PC-ClO_4-interaction. A broad band in

the range of wave number 1050 cm^{-1} - 1150 cm^{-1} appears to be a characteristic feature of PEO when combined with alkali metal salts or other materials. Symmetric and asymmetric stretching modes of C-O-C as well as CH mode are merged in this broad band. The peak at 1253 cm^{-1} is assigned to ether bonds of PEO; 1356 cm^{-1} and 1460 cm^{-1} are to C-H vibrations of different modes. The intense peak at 2246 cm^{-1} is due to C=N bond.

It is important to note that coordination between Li^+ ion and etherial oxygen of PEO chain exists suggesting the solubility of $LiClO_4$ in PEO in addition to its solubility in PC and EC. It is inferred that Li^+ ion is present in the HSPE in two different chemical environments. The distinction, however, is not reflected in impedance spectrum and ionic conductivity of the HSPE.

SEM micrographs of PEO + $LiClO_4$ and HSPE films are shown in Fig. 47. The morphology of PEO + $LiClO_4$ (Fig. 47a) is uniform throughout suggesting the formation of a homogeneous electrolyte. In Fig., 47b, long interlocked chains of PAN are clearly found. The liquid components viz., PC and EC containing $LiClO_4$ together with PEO are probably encapsulated in the cavities of the interlocked structure. This type of structure is perhaps responsible for retaining the liquid components within the film and keeping the surface of the film dry. The results on HSPE are published [12].

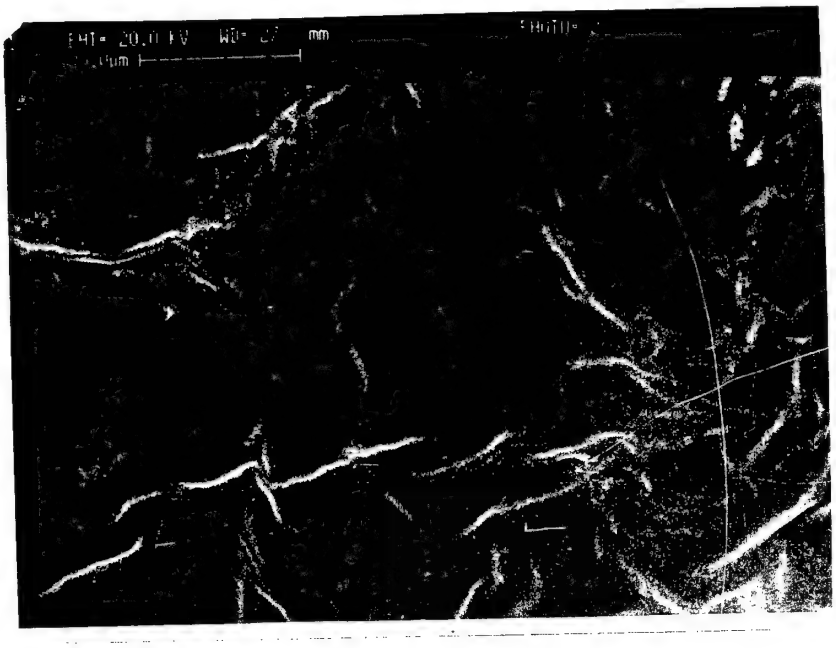

(a)

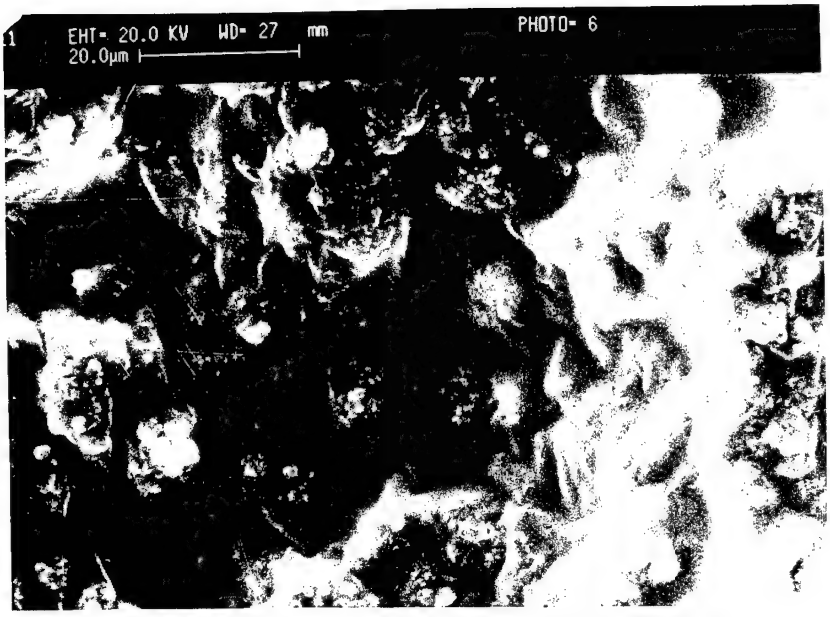

(b)

Figure 47. Scanning electron micrograph of (a) PEO +$LiClO_4$ film and (b) HSPE film.

4. CONCLUSIONS

(1) The electrochemical impedance spectrum of a lithium cell has been shown reflecting the passive film on lithium as well the charge-transfer reaction at the lithium/SPE interface.

(2) The specific conductivity of SPE, the resistance as well as the thickness of passivating layer on lithium, and the charge-transfer resistance and hence the exchange current density have been evaluated by analyzing the impedance data using Bouckamp non-linear least square fit procedure.

(3) Ageing of $Li/PEO_8LiClO_4/Li$ cells at ambient temperature as well as at 80°C revealed that the resistance parameters of the cell increase with ageing time.

(4) Ageing of Li/PEO_8LiClO_4-PC/Li cells at ambient temperature as well as at 80°C revealed the resistance parameters are very low when the cells were freshly assembled. However, the resistance values increase with ageing time and reach the values of $Li/PEO_8LiClO_4/Li$ cells.

(5) Specific conductivity of PEO_8LiClO_4-PC is as high as 5×10^{-4} S cm^{-1} in the initial stages of ageing. However, it decreases to about 1×10^{-6} S cm^{-1} in about 2000 h of ageing.

(6) Exchange current density in PEO_8LiClO_4-PC has been measured to be about 10 μA cm^{-2} in the initial stages of ageing. However, it decreases to a value of about 0.1 μA cm^{-2} in 2000 h of ageing.

(7) The resistance of Li/PEO_8LiClO_4-PC/Li cell increases at a rapid rate at 80°C, in comparison with the ageing behaviour of Li/PEO_8LiClO_4/Li. The faster rate of increase of R_{cell} is attributed to rapid growth of passive film on lithium in the presence of propylene carbonate.

(8) At 80°C, the exchange current in PEO_8LiClO_4-PC is about 0.2 mA cm^{-2} in the initial stages of ageing.. However, it decreases to about 0.1 mA cm^{-2} in about 200 h and remains nearly constant up to about 600 h of ageing.

(9) The resistance of passive film, charge-transfer resistance and hence the exchange current density are found to follow Arrhenius behaviour.

(10) The activation energies of R_f and I_o (or R_{ct}) decrease with ageing.

(11) Activation energies of the parameters do not have strong dependence on the concentration of propylene carbonate in PEO_8LiClO_4 electrolyte.

(12) Exchange current density of lithium electrode reaction does not follow kinetic equation with respect to its dependence on concentration of lithium salt in SPE.

(13) Galvanostatic voltage transient results suggest that transport of Li^+ ion through passive film on lithium metal is diffusion-limited when current flows through the cell.

(14) Dry, free-standing and dimensionally stable polymer electrolyte films with high ionic conductivity are prepared by a hybrid approach. The hybrid solid

polymer electrolyte film consists of poly(ethyleneoxide), poly(acrylonitrile), propylene carbonate, ethylene carbonate and lithium perchlorate.

(15) Optimization of the composition of HSPE was done by preparing several films with varying mole ratio of (PC+EC)/$LiClO_4$ and measuring the ionic conductivity at several temperature.

(16) Specific conductivity of optimized HSPE is 0.37 mS cm^{-1} and exchange current of lithium electrode reaction in HSPE is 1.3 μA cm^{-2} at 30°C.

(17) The energy of activation of conduction process in HSPE is 33.8 kJ mol^{-1}.

(18) Interfacial resistance at Li/HSPE is found to increase with ageing of the cells at ambient temperature.

(19) From IR spectra of HSPE films, it is inferred that coordination between Li^+ ion and etherial oxygen in polyethylene oxide exists suggesting the solubility of $LiClO_4$ in polyethylene oxide in addition to its solubility in propylene carbonate and ethylene carbonate.

(20) A study of SEM micrographs suggests that polyacrylonitrile forms a interlocked network of long chain of molecules which encapsulate the liquid components in its cavities. This type of structure is perhaps responsible for keeping the surface of the film dry.

References

1. "Lithium Batteries : new materials, developments and perspectives" ed. G. Pistoia, Elsevier, Amsterdam (1995).

2. "Lithium Batteries", ed. J.P. Gabano, Academic Press, NY (1983).

3. "Lithium Battery Technology", ed. H.V. Venkatasetty, John Wiley & Sons, NY (1984).

4. B. Scrosati in "Polymer Electrolyte Reviews-1", ed. J.R. MacCallum and C.A. Vincent, Elsevier, UK (1987) pp. 315.

5. N. Munichandraiah, A.K. Shukla, L.G. Scanlon and R.A. Marsh, J. Power Sources 62 (1996) 201.

6. A. Zaban, E. Zinigrad and D. Aurbach, J. Phys. Chem., 100 (1996) 3089.

7. F. Bonino, B. Scrosati, A. Selvaggi, J. Evans and C.A. Vincent, J. Power Sources 18 (1986) 75.

8. "Instrumental Methods in Electrochemistry", Southampton electrochemistry group, University of Southampton, Ellis Horwood Limited, U .K. (1985).

9. X. Wu, W. Zhang and H. Yu, J. Electroanal. Chem., 398 (1995)1.

10. G. Montesperelli, P. Nunziante, M. Pasquali and G. Pistoia, Solid State Ionics 37 (1990) 149.

11. A.M. Christie and C.A. Vincent, J. Appl. Electrochem., 26(1996) 255.

12. N. Munichandraiah, G. Sivasankar, L.G. Scanlon and R.A. Marsh, J. Appl. Polym. Sci. (1997) in Press.

LIST OF PUBLICATIONS

Some parts of the investigations are published in refereed journals. The details are given below:

1. On the stability of Li/PEO_8LiClO_4/Li symmetrical cells
   N. Munichandraiah, A.K. Shukla, L. G. Scanlon and R. A. Marsh
   J. Power Sources 62 (1996) 201- 205.

2. Characterization of PEO-PAN hybrid solid polymer electrolytes
   N. Munichandraiah, G. Sivasankar, L. G. Scanlon and R. A. Marsh
   J. Applied Polymer Science (1997) accepted.

FUTURE STUDIES

In literature, great importance has been given for studies related to ionic conductivity of solid polymer electrolytes. No doubt that it is an important area of research and development. An equally important area, viz., reaction kinetics in solid polymer electrolyte has not received a much attention. Future studies are intended towards this aspect. In brief, following are the objectives of the future studies.

(i) To evaluate exchange current density, energy transfer coefficient and related parameters of the lithium electrode reaction in several polymer electrolyte media. To establish correlation between the kinetic parameters and variable properties of the solid polymer electrolyte.

(ii) To study the influence of passive film formed over Li metal on the kinetic parameters of the reaction.

(iii) To study the effect of pre-treatment of lithium metal on the kinetics of the reaction and on film formation over lithium metal surface.

ACKNOWLEDGEMENTS

I am grateful to European Office of Aerospace Research and Development (EOARD), United States Air Force, London for financial support (Contract No. F61708-95-C007). My immense gratitude is due to Dr. Larry Scanlon and Mr. Richard Marsh of Wright Laboratory, USA for their encouragement to pursue this work. I thank Dr. M. Durga Prasad and Dr. T. S. Balasubramanian of Renewable Energy Systems Ltd., Hyderabad for providing cell fabrication facilities.

Dr. N. Munichandraiah.